UNIVERSITEIT VAN PRETORIA
UNIVERSITY OF PRETORIA
YUNIBESITHI YA PRETORIA

Faculty of Engineering, Built Environment and Information Technology

Fakulteit Ingenieurswese, Bou-omgewing en Inligtingtegnologie / Lefapha la Boetšenere, Tikologo ya Kago le Theknolotši ya Tshedimošo

University of Pretoria
Department of Chemical Engineering

Lead Biosorption Characterization of *Aspergillus piperis*: Contextualising the Novel Fungus Within the Larger Mycoremediation Corpus

Dissertation submitted in partial fulfillment of the requirements for the degree of M. Eng Chemical Engineering

Author

M. M. M. de Wet

2021-11-30

Lead Biosorption Characterization of *Aspergillus piperis*:

Contextualising the Novel Fungus Within the Larger Mycoremediation Corpus

Author: Martha Maria Marthina de Wet (26026946)
Supervisor: Hendrik Gideon Brink
Department of Chemical Engineering
University of Pretoria
Degree: Master of Engineering (Chemical Engineering)

Synopses

The Pb(II) adsorption capabilities of a heavy metal tolerant strain of fungus, *Aspergillus piperis*, were studied. Agar well diffusion was used with 2000 ppm of Cu(II), Fe(II), Pb(II), Mg(II), Mn(VI), Se(VI), Cd(II), and Zn(II) ions. Of the metals tested, *A. piperis* only exhibited substantial growth inhibition in Cd(II), while lesser inhibition was observed in Se(IV), Pb(II), and Zn(II). After five days the fungus had successfully grown in the presence of all the other metals. Optimal growth conditions were identified using a plating technique, and optimal adsorption conditions were identified using submerged fermentation and fractional factorial experimental design. The adsorption behaviour was then elucidated using isotherm and kinetic models, of which the one-surface Langmuir isotherm provided the best fit. The Langmuir maximum predicted adsorption capacity was 275.82 mg g^{-1}, which is similar to the experimental Q_{max} of 267.41 mg g^{-1}. Both these values are high when compared to other fungi tested for Pb(II) adsorption. Kinetic models suggested that internal mass transfer is the driving force behind the reaction rate. After adsorption, biomass surface characterisation was undertaken using ATR-FESEM, EDS, and FTIR suggesting that cation exchange is the underlying adsorption mechanism. The good adsorption performance as well as the relative ease in which this biomass can be manufactured indicate that *A. piperis* would be an excellent candidate for industrial Pb(II)-remediation.

Declaration

I, Martha Maria Marthina de Wet, declare that the work provided in this dissertation is to the best of my knowledge original (except where cited) and that this work has never been submitted for another degree at this or any other tertiary education institution.

M.M.M. de Wet
30 November 2021

A note about the figures

All photos, graphs, and illustrations are original work by M.M.M. de Wet.

Acknowledgements

- ∞ The National Research Foundation of South Africa (Grant Number: 121891).
- ∞ Dr. Deon Brink, for his supervision, optimism, unwavering support, encouragement, and meticulous proof-reading.
- ∞ The David de Wet Spousal Development Foundation for tuition fees and endless patience.

Contents

Chapter 1: Introduction

In 2018 a wild strain of fungus contaminated agar plates containing a consortium of lead-remediating bacteria at the Water Utilization Engineering Laboratory at the University of Pretoria, South Africa (Peens, 2018). The agar had a Pb(II) concentration of 80 ppm, which indicated that the offending fungus is lead-tolerant and could itself hold remediation potential. Peens (2018) isolated the fungus and conducted preliminary tests which suggested that the fungus can grow in the presence of Pb(II) and potentially lower the Pb(II)-ion concentration in the solution. Genetic sequencing identified the fungus as *Aspergillus piperis*, which is genetically distinct, but from the same clade as the better-known *Aspergillus niger*, colloquially referred to as "black mold".

This body of work is the continuation of these preliminary findings and represents an in-depth study of the potential lead-remediating properties of *Aspergillus piperis* in order to answer the research question: **Does *Aspergillus piperis* possess industrially useful Pb(II)-remediation properties?**

This dissertation starts with a literature study (Chapter 2) which contextualises *A. piperis* within lead (hereafter abbreviated as Pb to avoid confusion) mycoremediation, as well as within the larger field of bioremediation. While mostly phased out, Pb contamination still arises from industries like Pb-acid battery waste (Bhattacharyya and Banerjee, 2007) and – in South Africa in particular – illegal gold mining (Mathee, 2014). Toxic effluent waste treatment has recently seen a shift towards more affordable and sustainable practices such as bioremediation, the practice of using living organisms to promote remediation (Lehr et al., 2005). Bioremediation is generally achieved through isolation, immobilization, physical separation, extraction, or toxicity reduction of the xenobiotic substances (Berg, 2015). The primary mechanisms of bioremediation are described in the literature study chapter and include: Bioleaching, biotransformation, biodegradation, biomineralization, bioaccumulation, and biosorption (Atlas and Philp, 2005), which is typically utilised by fungi.

Mycoremediation, the term given for bioremediation which uses fungi, has enjoyed much focus in remediation research recently as their myriad of industrial applications become elucidated (Bhandari et al., 2007). Fungi are good propagators, have numerous physical advantages over other biological remediators, and produce a seemingly endless host of metabolites (Zhou and D Li, 2018), all of which allows them to compete with commercial remediation practices. Examples of such mycoremediators include wood decay fungi, mycorrhizal fungi, and molds like those in the *Aspergillus* genus. This genus has proved

capable of heavy metal remediation including Pb adsorption, and as part of this genus, *A. piperis* is studied to determine whether it holds those same properties.

After the literature study, experimental work was undertaken to test the heavy metal tolerance of *A. piperis* (Chapter 3). The aim of this chapter was to gauge whether the fungus could be used in industrial remediation practices by establishing a preliminary list of heavy metal environments in which it can survive, as well as to confirm growth in the presence of Pb(II). To identify these habitable environments for the fungus, metal solutions were introduced to the center of an inoculated agar plate, using the simple and cost-effective agar well diffusion method (Xie et al., 2005). The agar well diffusion method was used with metal solutions containing 2000 ppm of copper (Cu(II)), iron (Fe(II)), lead (Pb(II)), magnesium (Mg(II)), manganese (Mn(VI)), selenium (Se(VI)), cadmium (Cd(II)), and zinc (Zn(II)) ions.

Once it was established that the fungus is tolerant to Pb, its preferred growth conditions were determined, once again using agar plates (Chapter 4). This time the potato dextrose agar was mixed with either Pb or acid to get a range of pH and Pb environments. A small amount of spores was then placed in the middle of each plate and radial mycelial growth was measured daily. Based on these findings, submerged fermentation was used to gauge what adsorption capacity the living fungus can display, and sacrificial sampling was used to get intermediate information about the adsorption process. For more controlled experiments, the mycelium was grown, drained, and dried so that the dead biomass capabilities could be quantified more accurately in the effort to find optimal adsorption conditions. To simplify the process of testing factors such as pH, initial Pb, temperature, and biomass preprocessing, fractional factorial design was used.

After finding optimal biomass growth and adsorption conditions, in-depth adsorption studies were conducted using dried biomass (Chapter 5). To quantify the observed adsorption, the data was fitted to various mathematical models in order to explore the underlying adsorption mechanisms. Isotherm studies, where adsorption equilibrium is reached at constant temperatures, was used to characterise the adsorption surface types. The models used for these studies were the one- and two-surface Langmuir, as well as the Freundlich isotherm. Kinetic adsorption studies were also conducted at constant temperatures, but samples were taken at intervals to obtain information about the adsorption rate. These kinetic studies provided information about the rate limiting steps during the adsorption process. For general rate descriptions, the empirical pseudo-first-order, pseudo-second-order, and two-phase models are used. To compare external and internal diffusion rates, the Mathers and Webber model, combined with an adaptation of the Crank model is used. Finally active site adsorption rates were described using the Langmuir kinetic model.

To understand what mechanism is responsible for adsorption, the dried biomass surface was characterised to study the effect of Pb(II) adsorption on the fungus morphology (Chapter 6). Particle morphology was studied using ultrahigh resolution field emission scanning electron microscopy (FESEM), which was then fitted with an energy dispersive X-ray spectrometer (EDS) to identify elemental compositions of specific sites on the mycelium. Finally fourier transform infrared (FTIR) spectroscopy was recorded before proposing potential adsorption mechanisms based on surface characterisation data and literature.

Chapter 2:
Literature Study

The aim of this chapter is to contextualise *Aspergillus piperis* within the field of mycoremediation. This section is an abbreviated version of Chapter 18: Fungi in the Bioremediation of Toxic Effluents, published in the book *Fungi Bio-Prospects in Sustainable Agriculture, Environment and Nano-technology* in February 2021 (de Wet and Brink, 2021a) with co-author Dr. H.G. Brink.

2.1 Industrial toxic effluent

During industrial processes, liquid runoff, otherwise known as effluent, is often discharged into nearby bodies of natural water, and frequently contains significant amounts of polluting by-products. These include synthetic dyes, pesticides, polychlorinated biphenyls and a host of metallic compounds (Bhandari et al., 2007). Mining is a major source of toxic effluents but by no means the only one. Pesticides, sanitation, textile industries, municipal waste incinerators, smelting industries, fertilizers, and sewage (Bhandari et al., 2007) are only some of these sources.

Although many metals, such as calcium, copper, chromium, cobalt, iron, potassium, magnesium, manganese, sodium, nickel and zinc are essential to most living organisms (Rathoure and Dhatwalia, 2016) including humans and animals, ingesting high dosages could be harmful. On the other hand, toxic metals like cadmium, mercury and lead are generally of no biological use and should never be ingested. The effects of these heavy metals on humans and animals are largely dependent on the amount of metal inside an organism at any one time. Pb, for example, is a cumulative toxin, with both acute and chronic exposure resulting in a host of symptoms such as headaches, fatigue, renal failure, or death (Ngo et al., 2016).

Pb occurs naturally in almost all rock at concentrations around 2 – 200 ppm (Lehr et al., 2005), but anthropogenic activities have greatly increased human and animal exposure to this metal. Although ideally zero, the permissible blood serum Pb level for a child is 5 μg dL^{-1} (CDC, 2012) and values higher than this have been associated with hearing loss, lowered intelligence, aggression, and violent behaviour (Harper et al., 2003), while acute exposure can result in organ failure and death.

Although Pb is being phased out of common industrial practices such as Pb-based paint and leaded petrol (Lehr et al., 2005), much of the contamination of the past remains while

other industries continue to exacerbate environmental exposure to Pb. One source of this is Pb-acid batteries: While these batteries are the most efficiently recycled commodity in the world (Berg, 2015), many of them still end up in landfills where they leach into the ground. Because Pb tends to accumulate in living organisms, organisations such as the United States Environmental Protection Agency (EPA) suggests that the permissible Pb in industrial effluent should be zero (Mackenzie and Davis, 2020). In South Africa human exposure is often associated with informal industries like illegal gold mining, battery salvaging, and the use of Pb sinkers for subsistence fishing (Mathee, 2014).

Pb water treatment usually falls into one of the following categories: adsorption, electrodialysis, precipitation, membrane filtration, evaporation, and ion exchange (Sahoo and Prelot, 2020). Industrial water treatment commonly utilises carbonate or hydroxide treatment because the Pb can be recovered through filtration, but this method is expensive and requires long retention times (Ecolab, 2018). More recently new techniques have been developed whereby remediation is carried out via biologically active compounds.

2.2 Bioremediation of toxic effluents

Ideally xenobiotic substances (a chemical that is foreign and possibly harmful to an environment) should be contained and never released into nature, yet inadvertent toxin contamination still occurs, and large industries are built on remediation strategies. Lehr et al. (2005) groups these remediation strategies into five general categories: Isolation, immobilization, physical separation, extraction, and toxicity/mobility reduction. The latter often makes use of biological treatments such as bioremediation.

Bioremediation is a method of removing xenobiotic compounds by using living organisms such as plants, fungi, algae, and bacteria. This holds numerous benefits over other techniques, like low operating costs, high efficiency, and the possibility of metal recovery (Bhattacharyya and Banerjee, 2007), despite limitations like microbial mutation and inadequate supply of nutrients (Rathoure and Dhatwalia, 2016).

Bioremediation is often less expensive, less water-intense, and there is less sludge runoff (E Priyadarshini, S Priyadarshini, and Pradhan, 2019). In addition to this, bioremediation can be applied to small scale remediation efforts with low startup costs (Sao et al., 2017). Examples of bioremediation for Pb treatment can be found in plants, such as *Tinospora cordifolia* with Pb adsorption of up to 63.77 mg g^{-1} in an hour (Sao et al., 2017); or moss, like *Stereophyllum radiculosum* with with Pb adsorption of up to 12.5 mg g^{-1} in 50 minutes (Babarinde et al., 2010); and even fungi.

2.2.1 Mechanisms and examples of bioremediation

Atlas and Philp (2005) describes some of the most common microbial interactions that occur during bioremediation as bioleaching, biotransformation, biodegradation, biomineralization, bioaccumulation, and biosorption. A summary of how a fungal cell would interact with a metal ion using these mechanisms can be seen in figure 2.1.

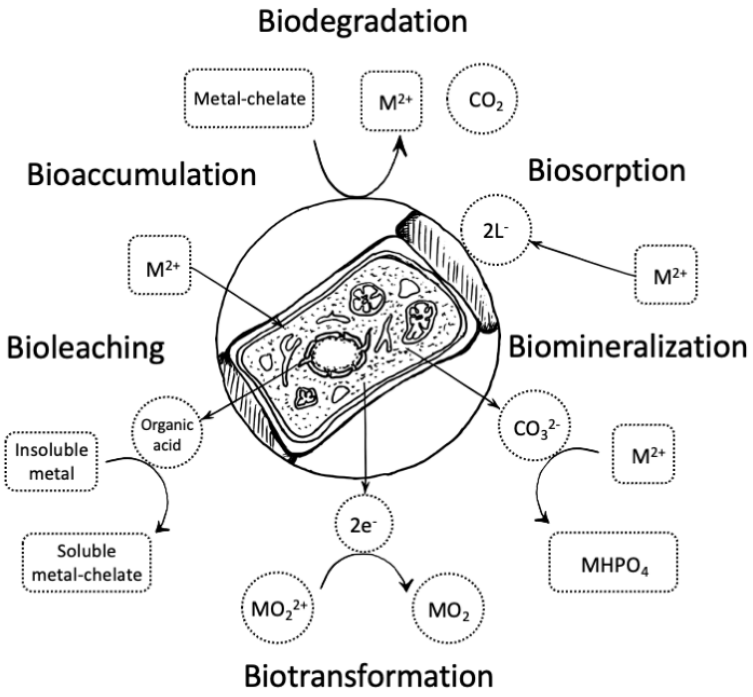

Figure 2.1: Mechanisms of fungal cell interactions with metal ions (adapted from Atlas and Philp, 2005, p. 295).

2.2.1.1 Bioleaching

According to Brandl (2001), bioleaching occurs when metals are mobilized out of solid materials through ligand-induced metal solubilization. Examples of such ligands can be organic acids which are often used to recover minerals from sources like sewage sludge, spent batteries, fly ash, electronic scrap metals, amongst others (Marafi et al., 2017). Some of the most common organisms to do so are in the *Acidithiobacillus*, *Aspergillus* and the *Penicillium* genera, for example *Penicillium simplicissimum* being used to extract elemental Zn from ZnO (Bhandari et al., 2007). Fungi is also particularly excellent at phosphorus bioleaching, where organic acids such as citric and oxalic acid solubilize phosphorus from Fe and Al phosphates. In this process carboxylic anions compete with bonding sites which chelates Al^{3+} and Fe^{3+} (Lu, 2015).

Some advantages of bioleaching would be that it tends to be environmentally friendly with low energy requirements and minimal emissions (Jafarinejad, 2017). It is also relatively simple and easy to maintain and does not require very specialised environments to function. Although abiotic chemical processes have a much quicker process time, bioleaching can work in highly contaminated sites and have a higher metal removal efficiency.

In a study by Marappa et al. (2017), precious metal recovery from electronic waste using *Aspergillus niger* was studied where printed circuit boards were ground up into a fine powder which made up 0.1, 0.5 and 1 % of a solution with 10 % inoculum. The pH, particle size, and pulp density were varied to find optimal conditions for metal recovery. The primary metals present were Ag, Cu, Fe, Hg, Br and Si. The process worked best in low concentrations of electronic waste and Ag, Cu, and Fe concentrations in solution

increased, which implies that bioleaching of the metals took place.

Fungal species were isolated from abandoned sulphide mines in Italy by Cecchi et al. (2019): Two *Penicillium fungi*: *P. brevicompactum* and *P. glandicola*, as well as a strain of *Trichoderma harzianum* were tested for pyrite-chalcopyrite mineralization, mineral bioleaching and metal accumulation and managed to grow in highly acidic conditions where the pH was often in the region of 2. *T. harzianum* displayed the highest capacity to bioconcentrate Ag, Cu, Cd and Zn. Adding these fungal species to sulphide mine effluent substantially accelerated sulphide mineralization, while the control showed no mineralization.

2.2.1.2 Biotransformation

Biotransformation occurs when the microbe excretes catalytic enzymes. In this process a redox reaction takes place where a toxic substance such as a metal can be transformed into a more volatile or less soluble form (Atlas and Philp, 2005, p. 294). An example of this is reducing Hg (II) to Hg (0) which can then be diffused out of a cell and transported away (Bhandari et al., 2007, p. 736). It is also an excellent method of recovering precious metals, and the reaction can take place in the presence of a living or dead cell, as long as adequate catalytic enzymes are present. With biotransformation it is possible to promote site- and sterio-specific reactions, which are sometimes impossible to do chemically (Kück and Frankenberg-Dinkel, 2015), and molds in particular can achieve specific reactions though hydrolysis, isomerization, and condensation. In addition to this, fungi can often excrete specific enantiomers, whereas chemical processes tend to produce enantiomers in equal amounts.

A common application of biotransformation is in the production of steroids: one million tons of steroids are produced globally every year with hydroxylation as the most prominent type of conversion (Kück and Frankenberg-Dinkel, 2015). There are three main approaches to biotransformation (Bhattacharyya and Banerjee, 2007), namely using growing cells, with washed/resting cells, or with immobilized biocatalysts. Advantages of biotransformation are the high chemo-, regio-, and sterio-selectivity, the cost-saving benefits of requiring mild reaction conditions, minimal side reactions, and easy separation (Flickinger, 2010).

2.2.1.3 Biodegradation

Biodegradation uses the decaying abilities of microbes to transform a material into a safer or more useful form by allowing the microbes to break the offending agents down into simpler components because polymers with long chains can't penetrate microbial cell membranes and be utilized by the organisms. This process can be broadly categorized into three steps. First biodeterioration takes place where mechanical, thermal, ultraviolet, and other abiotic processes break down long polymer chains into shorter segments. Next bio-fragmentation takes place where deterioration continues but now microbes also secrete intracellular and extracellular enzymes that further break down polymers into monomers and oligomers (Al-Salem, 2019). Finally assimilation takes place where the microbes use monomers to form energy, create new metabolites, and form biomass. Another process that takes place during assimilation is mineralization where monomers not used by microbes escape as gas molecules and salts are excreted into the environment

(Falkiewicz-Dulik et al., 2015).

This ability to degrade polymers is especially important in the endeavour to remove pollutants from large water sources such as the ocean. The marine fungus, *Zalerion maritimum*, uses these mechanisms to degrade polyethylene-based microplastics in the ocean as a source of nutrients (Paco et al., 2017).

2.2.1.4 Biomineralization

Biomineralization is an extremely common phenomenon in nature, and occurs when an organism uses mineral compounds such as carbonates, silicates, and phosphates to support their biological structures. An example of this is sea shells, but even microorganisms such as *Phanerochaete chrysosporium*, a type of white rot fungi, can remove Se and Te from effluent though biomineralization (Espinosa-Ortiz et al., 2017). The process is promoted by the fungus' mycelial matrix which regulates nucleation and development of the mineral structures (Q Li and Gadd, 2017). This nucleation, also referred to as a priming deposit, acts as a host crystal for metal to further precipitate around. Atlas and Philp (2005) describe this secondary process as a form of microbially enhanced chemoabsorption. Artificially creating such nano-structures for industrial purposes is incredibly difficult, making microbial biomineralization a much cheaper and more efficient option.

An important function of biomineralization is the treatment of uranium contaminated groundwater which involves the precipitation of uranium phosphate minerals. In this process negatively charged ligands, excreted by microbes, attract uranyl ions, UO_2^{2+}. When this happens autunite, $Ca(UO_2)_2(PO_4).10\text{-}12H_2O$, forms – a compound less mobile than UO_2^{2+}. An advantage of microbial ligands is that the ligands will specifically react to uranium and not to other metals in the solution. Because this process occurs at the cell surface, nucleation further drives these reactions. Some challenges in these types of remediation processes are microbial inhibition of U(VI) in the presence of nitrate and the inherent instability of U(IV) in the mineral phase which may undergo further redox reactions under aerobic conditions.

2.2.1.5 Bioaccumulation

Bioaccumulation is a broad term that generally describes the incremental uptake of specific chemicals by an organism, for example when mercury moves up the food chain in fish. In microbes such as fungi this also takes place when a toxicant enters a cell through metabolic cycles (Rathoure and Dhatwalia, 2016), an energy dependent process where the toxin acts as a chemical surrogate. There are many other mechanisms whereby toxins can accumulate in mycelium through direct contact, namely: Ion-exchange, electrostatic attraction, complexation, adsorption, van der Waal forces, and precipitation (Mathew et al., 2015). While the bioaccumulating property is useful for remediation because it draws toxins out of a substrate, edible fungi like oyster mushrooms (*Pleurotus ostreatus*) can accumulate these toxins in their fruiting bodies and should not be eaten (Stamets, 2005).

Endophytic fungi reside inside a plant's tissue and form a symbiotic relationship with the plant. Soleimani et al. (2010) studied *Neotyphodium* endophytes found inside two *Festuca* grass species. Hydroponic systems were used with 0, 10, 20, 40 mg L^{-1} Cd solutions,

and up to 16 and 20 % more of the Cd was accumulated in the plant roots and shoots, respectively, when compared to the control grass which wasn't inoculated.

Wastewater from industries such as electroplating and tanning often contain plenty of heavy metals. Joshi et al. (2011) studied metal tolerance and bioaccumulation properties of 76 fungi found in contaminated wastewater, as well as in *Phanerochaete chrysosporium*, *Trichoderma viride*, *Aspergillus flavus* and *A. awamori*. The majority of the fungi could tolerate up to 400 ppm Pb, Cd, Cr and Ni while the maximum metal accumulation for each of the four tested fungi was: 59.67 mg g^{-1} Pb in *A. terrus*, 16.25 mg g^{-1} Cd in *T. viride*, 0.55 mg g^{-1} Cr in *T. longibrachiatum*, and 0.55 mg g^{-1} Ni in *A. niger*.

2.2.1.6 Biosorption

Adsorption is a surface phenomenon, where a substance (adsorbate) is collected at an interface (adsorbent) and is often accompanied by ion-exchange reactions. Chemical sorption is driven by strong chemical associations, while physical sorption is driven by weaker van der Waal intraparticle interactions. These processes are usually temperature dependent to some extent, and fairly rapid. A wide variety of binding groups are usually involved in metalloid adsorption such as carboxyl, amine, hydroxyl, and phosphate groups (Naidu et al., 2006).

While Similar to bioaccumulation, biosorption differs in a critical way: Bioaccumulation is always associated with living organisms, whereas biosorption is a passive uptake of toxins that occurs on the cell surface, whether the organism is dead or alive (Rathoure and Dhatwalia, 2016). Because the reactions occur on the surface of cells, the magnitude of biosorption is directly proportional to the density of the biomass available. Fungal products that promote biosorption include chitins, chitosans, glucans, and mannans. Some biosorption mechanisms are redox reactions that can either be assimilating reactions, where microbes assimilate compounds needed for protein formation; or disseminating, where the metal substitute plays no significant physical role in the organism's wellbeing. Other mechanisms involve methylation and demethylation, which can result in a change in compound solubility, volatility, mobility, and toxicity.

Penicillium simplicissimum removes chromium from solution when live biomass is used (Chen et al., 2018), while dead *Aspergillus niger* removes chromium from wastewater (Vale, 2016), both though biosorption. Hansda et al. (2016) considers biosorption superior to bioaccumulation for a number of reasons, but primarily because biosorption does not involve toxins being absorbed into the cells, which means that the fungus won't be overwhelmed by the toxin and die. Bhattacharyya and Banerjee (2007) describe other advantages of biosorption: It is more effective than physio-chemical methods at removing low concentrations (2 – 10 ppm) and the organism is not hampered by alkaline earth metals as seen during ion-exchange reactions.

Dye wastewater is an effluent that often contains a lot of recalcitrant toxic compounds. Rybczynska-Tkaczyk and Korniłłowicz-Kowalska (2016) tested two strains of *Haematonectria haematococcus*, as well as *Trichoderma harzianum* for their biosorption capabilities in the presence of the dye Alizarin Blue Black B, and alkali lignin, both of which are common in textile industries. The optimal conditions for biosorption were 1 mg L^{-1} biomass, with a pH of 7 at 28 °C. The *H. haematococcus* species had the best adsorption capacities at 247.47 mg g^{-1} and a Freundlich isotherm relation was determined with K_F

= 28.20 and n = 3.46.

2.2.2 Mycoremediation

Fungi play a major role in bioremediation, even on large-scale commercial levels (Bhandari et al., 2007) by converting toxic compounds into more benign chemicals, or immobilizing harmful compounds. When fungi is used for bioremediation, it is referred to as mycoremediation, and applications such as fungal filters are of particular use because they are cheap and readily available (Price et al., 2001). Factors to consider when using mycoremediation are selecting the fungal species to use, how the area will be inoculated, and whether any surfactants are required to increase the bioavailability of the pollutants. These decisions are usually made beforehand based on laboratory trials (Hurst et al., 2007).

To explain why fungi are such good bioremediators, it is helpful to look at their role in nature. Firstly, their unique physiological characteristics make them excellent chemists: The filamentous mycelium gives them the ability to slowly explore their surroundings uninhibited in search of new substrates, unlike bacteria, whose movement is largely dependent on outside factors such as fluid movement and direct contact. This means that fungi can explore different types of environments, making them often more tolerant to toxins than bacteria and other microorganisms (Hurst et al., 2007). Secondly, they produce a myriad of metabolites to control their environments.

Factors affecting fungal adsorption are pH, metal-ion to biomass ratio, cell-wall fraction, presence of ligands, and temperature to a lesser extent (Zhou and D Li, 2018), (E Priyadarshini, S Priyadarshini, Cousins, et al., 2021). Fungi also perform well when compared to commercial heavy metal treatment like ion-exchange resins, activated carbon, and metal oxides, and the biomass can often be recovered after desorption (Kapoor and Viraraghavan, 1995), (Yousefi et al., 2021). Mycoremediation for Pb can come in the form of mushrooms, such as *Lepiota hystrix* which demonstrated Pb adsorption of up to 8.90 mg g^{-1} in 40 minutes (Kariuki et al., 2017), and molds (Khan et al., 2019).

2.2.2.1 Wood decay fungi

White rot fungus (WRF) is a general term used to describe a type of saprophyte that digests wood, rotting it in the process. It is perhaps the most studied fungus in bioremediation (Bhandari et al., 2007), with *Phanerochaete chrysosporium* as the first WRF to be tested for widespread remediation potential and is still widely used in paper industries for biopulping.

To digest wood, WRF requires an extensive menu of enzymes to break down cellulose, hemicellulose and, most importantly, lignin. These non-specific, extracellular, and highly oxidative enzymes are part of a complex lignin-degrading system which can oxidise a wide variety of hydrophobic pollutants such as polyaromatic hydrocarbons, high-molecular-weight organic compounds, polychlorinated dibenzo-p-dioxins, and polychlorinated dibenzofurans (Hurst et al., 2007). Because these pollutants are generally not used as a fuel source by WRF, their concentrations don't affect the fungus' ability to thrive — as long as there is enough substrate and as long as the fungus can tolerate the presence of the toxin, it will continue to grow and remediate its surrounds, regardless of the amount of toxin in the vicinity.

The primary mechanisms whereby WRF remediate their environment is directly, through lignin-degrading enzymes that oxidises pollutants; as well as indirectly, when ligninolysis results in transformation and mineralisation (Hurst et al., 2007). The fungus also produces quinones, which reduces heterogenous aromatic lignin structures, and thus have a similar effect on aromatic pollutants such as polycyclic aromatic hydrocarbons and polychlorinated biphenyls.

2.2.2.2 Mycorrhizal fungi

Endophytes are microorganisms that live between plant cells, often populating the soil surrounding plant roots, forming a symbiotic relationship with the plant. Phytoremediation is the use of plants to remediate contaminated soil or water, but most plants aren't as resistant to toxins as their endophytes are. For example, endophytes can produce compounds such as salicylate, which facilitates the removal of polycyclic aromatic hydrocarbons (Rathoure and Dhatwalia, 2016).

This symbiotic fungi-plant relationship is referred to as the mycorrhiza, and takes place in the plant's rhizosphere (root system). Because mycorrhizal fungi live in symbiosis with its host plant, it is in their interest to ensure that the plant is healthy and thus it assists in many housekeeping functions. The mycorrhizal fungi can either play an extracellular role, such as ectomycorrhizal fungi, which forms what is known as a Hartig net around the plant's roots, or it can be intracellular, as with arbuscular mycorrhizal fungi (AMF), an important component to plant health.

AMF have unique structures, called arbuscules, which have a host of functions including helping a plant capture nutrients. These incredible fungi are found all over the world, in almost any climate or conditions where plants exist, including heavily polluted and toxic sites. Species are usually isolated from such mine/industrial waste sites and selected for their xenobiotic resistance so that they can be used to inoculate other plants (Zaidi et al., 2012), although they can't be cultivated in the absence of plants for a meaningful amount of time (Frossard et al., 2006). Over 80 % of vascular plants are known to make use of AMF in some form, and the complex symbiotic interaction holds numerous benefits to the plant, much of which is still being discovered. A primary function of AMF in a plant is to assist with nutrient uptake, facilitating the intake of essential metals such as Cu, P, Zn and N, while limiting others like Fe, Mn and Al (Frossard et al., 2006). The fungi also modulate plant resistance to external stresses like pathogens, and the mycelial network assists with mechanical soil stabilization. Informal observations of plants mysteriously thriving under traditionally hostile conditions has inspired much research and AMF has often been found to be responsible for the plants' resilience. Examples of this is maize and barley thriving in a heavy metal contaminated site in Germany, where conditions would be deadly to the plants in the absence of AMF (Frossard et al., 2006). The same is observed in North America with excess Zn. AMF behaviour has been tested in the presence of metals such as Zn, Cd, Pb, to name but a few, as well as radioactive isotopes of Cs, U and Sr. The results from these studies vary, and the species of fungi, plant species, conditions and previous exposure to the toxins all play a role in the fungi's tolerance, but in general, heavy metals do harm AMF, although less so than their host plant, and much less once the fungus has had time to develop resistance to it.

2.2.2.3 Molds and other filamentous fungi

Outside the world of mycology and French cheese, mold is generally considered a pest. Yet there are several species of mold that are invaluable in industry such as antibiotic *Penicillum* molds and *Aspergillus oryzae*, which is used in the fermentation of soy sauce, and rice wine (Adams et al., 2016). Mold is a broad term that colloquially refers to multicellular filamentous fungi — unlike unicellular yeasts. Most molds are from the *Ascomycota* phylum, and unlike saprophytes and mycorrhizal fungi, are much less selective about their food sources. These fungi will primarily digest sugars, proteins and lipids (Kuntz, 2018), but many molds are oligotrophs (an organism that can survive on very little nutrients), and often make-do with unconventional food sources. While molds don't produce fruiting bodies, they can be easily recognised visually by the fuzzy appearance of their spores, and most species can be identified microscopically by hyphae and spore characteristics.

Because of mold's propensity to use a wide variety of organic materials as substrate, they are prolific producers of bespoke metabolites. These include fumaric acid, citric acid, oxalic acid, alcohols, amongst many other compounds, including mycotoxins (toxic compounds secreted by fungi) such as aflatoxin, which is produced by *Aspergillus flavus* when peanuts are used as a substrate. Mucor mold mycelium have the distinct appearance of being covered in droplets of water, which are in fact copious amounts of secondary metabolites being excreted.

Mold's ability to thrive in hostile environments can even be illustrated by poisonous wallpaper. In the 19$^{\text{th}}$ century, a cupric hydrogen arsenite ($CuHAsO_3$) was used as a popular grass-coloured paint pigment, named Scheele's Green. Fungi from the genera *Scopulariopsis* and *Paecilomyces* often grew on such green, arsenic-laden wallpaper (Naidu et al., 2006). For years Europeans were struck down with vomiting, abdominal pain, and death — typical arsenic poisoning symptoms — until Bartolomelo Gosio discovered that mold on the wallpaper was emitting trimethylarsine, which he named "Gosio gas". Arsenic use as a pigment was eventually discontinued, but not before supposedly contributing to Napoleon's death. Thus it comes as no surprise that *Scopulariopsis brevicaulis* has been shown to thrive amidst arsenic in modern studies (Andrews et al., 2000).

2.2.2.4 Molds: Aspergillus

Aspergillus is one of the most studied, and industrially important fungi genera, producing a variety of important enzymes such as citric acid, gluconic acid, itaconic acid, kojic acid as well as secondary metabolites like the life-saving cholesterol-lowering drug, lovastatin (Gupta, 2016), which is produced by *A. terreus* (Robinson, 2000), and prescribed 7 million times per year (NCBI, 2017). Estimates periodically increase, but as of 2018 there are over 300 species of *Aspergillus*, of which only three are known to cause serious disease: *A. flavus*, *A. terreus*, and *A. fumigatus*, and even then it is mostly opportunistic (WEF, 2017). The vast majority of *Aspergillus* fungi thrive incognito all over the world without doing much more damage than occasionally spoiling food. And also occasionally improving food: *A. oryzae* and *A. sojae* are both critical culinary components in Asian cuisine. Koji, the solid state fermentation of these molds on cereals like rice, barley and wheat, and is used to produce food such as miso, soy sauce and sake (Robinson, 2000).

Bano et al. (2018), amongst others, have done extensive research on the heavy metal

remediation potential of the *Aspergillus* group, namely *A. gracilis*, *A. penicillioides*, *A. flavus*, *A. penicillioides*, and *A. restrictus*. 1 000 ppm of Cd, Cu, Fe, Mn, Pb, and Zn were added to potato dextrose broth, inoculated and incubated for two weeks. All the fungi displayed high levels of adsorption with *A. flavus* adsorbing 86 % of the metallic mixture and *S. halophilus* 83 %. The metals of which the most were removed were Fe and Zn. This genus has been extensively studied with respect to Pb remediation in particular (Tang et al., 2021): *A. Fumigatus* demonstrated Pb adsorption capacity of up to 43.7 mg Pb(II) per g^{-1} while *A. versicolour* adsorbed to 45.0 mg g^{-1} in three hours (Bairagi et al., 2010), and *A. parasiticus* adsorbed 83.3 mg g^{-1} in 70 minutes (Akar et al., 2007), to name but a few.

2.2.2.5 Molds: Aspergillus niger

Another member of the *Aspergillus* genus is *A. niger*, commonly referred to as "black mold" when found on onions by dismayed cooks around the world (figure 2.2), easily identifiable by its black spores, which protects it from ultraviolet damage (Doyle and Buchanan, 2013). Despite its notoriety as a home-invader, this ubiquitous little workhorse is the primary producer of over 1.6 million tons of citric acid per year (Show et al., 2015), and has been shown to remediate a host of xenobiotics, from aluminium (Boriova et al., 2019) to zinc (Vale, 2016). The proposed mechanism whereby *A. niger* would remove metals from effluent is biosorption.

Figure 2.2: Produce such as onions typically harbor the *A. niger* fungus.

2.3 *Aspergillus piperis*: a newly identified member of the *A. nigri* group

2.3.1 *Aspergillus piperis* contamination at the University of Pretoria laboratories

In 2018 a wild strain of fungus contaminated a set of agar plates containing 80 ppm of Pb in the Water Utilization Engineering Laboratory at the University of Pretoria, South Africa. The fungus was isolated and preserved for further research (Peens, 2018). Preliminary tests suggested that the fungus survives in the presence of Pb(II) while simultaneously lowering the metal ion concentrations in solution (de Wet, 2019). Genetic sequencing identified the fungus as *Aspergillus piperis*. The fungus mycelium is white, and though it produces no fruiting bodies, it has the same characteristic distinctive black spores of a *A. niger* fungi.

2.3.2 *Aspergillus piperis* in literature

While *A. niger* is a species of fungus on its own, recent genomic analysis has revealed that the *Aspergillus* group has numerous fungi that resemble *A. niger*, but are genetically distinct. These fungi fall within the *Aspergillus nigri* group, which *A. niger* shares with around 25 other species (Varga et al., 2011). One such a fungus is *Aspergillus piperis*, a black mold originally isolated from peppercorns, and was first described by Samson et al. (2004) in 2004, and its genes were sequenced along with other *A. nigri* species in 2018 (Vesth et al., 2018). Because of the relatively recent genomic identification of *A. piperis* it is possible that the fungus may have formed part of other studies, mistakenly identified as *A. niger*. For example a consortium of fungi might show certain capabilities such as producing the mycotoxin, fumonisin, but when Onami et al. (2018) separated *A. niger* from other black mold, including *A. piperis*, *A. niger* was the only fungus which produced fumonisin. At this stage studies specifically targeting *A. piperis* are severely limited and the fungus is primarily considered for its pest-controlling capabilities.

A. piperis does not like sharing its substrate with other fungi and has developed a host of metabolites to ward off others. Jovicic-Petrovic et al. (2016) studied this property by collecting compost which inhibits *Pythium aphanidermatum*, an oomycete (a fungus-like water mold) which causes plants to rot. In the compost, microbes were isolated and *A piperis* was identified as the key organism responsible for the anti-oomycete properties. Further testing revealed that these antagonistic properties were driven by *A piperis'* ability to excrete anti-fungal organic solvents, heat-resistant proteins, as well as gluconic, citric, and itaconic acid.

In 2017 Eldebaiky (2017) isolated *A. piperis* from produce such as tomatoes and onions and tested the fungus' antagonistic behaviour towards phytopathogenic fungi such as *Sclerotinia sclerotiorum*, *Sclerotium cepivorum*, *Alternaria alternate*, *Alternaria solani* and *Botrytis cinerea* in vitro. In this study *A. piperis* was placed with each of the other fungi, one-by-one, on agar plates and successfully suppressed their growth every time. Compared to another well-documented and widely used antifungal, *Trichoderma harzianum*, *A. piperis* performed much better, with its best result an 81.85 % fungal

inhibition, while *T. harzianum* could only manage 45.18 % inhibition. Inspired by these results, Eldebaiky (2018) conducted another study in 2018 where early tomato blight, caused by the fungus *Alternaria solani*, was studied as a target for *A. piperis*' antagonistic capabilities. They found that by applying *A. piperis* spores to the tomato leaves, the plants only had 10.25 % chance of contracting blight, which is lower than the control rate of 25 %.

Aspergillus piperis shows promise in the field of pest control, however after the lab contamination in 2018 another potential application for this promising fungus came to light: Heavy metal remediation. This thesis adds to the corpus of Pb remediating *Aspergillus* species by bioprospecting *Aspergillus piperis* for Pb(II) adsorption.

Chapter 3:
Heavy Metal Tolerance

The aim of this chapter was to confirm that *Aspergillus piperis* can survive in the presence of high Pb(II) concentrations, and to find out whether the same is true for other heavy metals. This section is based on a manuscript published in the journal *Chemical Engineering Transactions* in April 2020 (de Wet, Brink, and Horstmann, 2020) with co-authors Dr. H.G. Brink and C. Horstmann.

3.1 Materials and Methods

3.1.1 Reagents used

A. piperis, like most *A. niger* fungi, had already exhibited the ability to thrive in potato dextrose agar (PDA) (Dynowska et al., 2011). PDA from Merck KGaA (Darmstadt, Germany), was prepared according to the manufacturer prescribed method of 39 g L^{-1}. Pb(II), Cu(II) and Zn(II) were chosen for their occurrence in industrial effluents, especially in mining (Wei et al., 2019), and the remaining metals were selected according to laboratory availability. The dry reagents used were: 1.598 g $Pb(NO_3)_2$, 2.952 g $Cu(NO_3)_2$, 2.896 g $Zn(NO_3)_2$, 4.037 g $CoCl_2.6H_2O$, 2.720 g $FeSO_4$, 3.918 g $MgCl_2$, and 3.076 g $MnSO_4.H_2O$.

The dry reagents were each dissolved in 100 mL distilled water, after which they were serially diluted to the desired concentration of 2 000 ppm. Stock solutions of Se(VI) and Cd(II) were readily available at a concentration of 10 000 ppm and were also diluted so that all metal solutions had a final concentration of 2 000 ppm metal ions. The metal concentrations were chosen so that the PDA would have a maximum concentration of 2 000 ppm and a minimum of 280 ppm during the agar well diffusion. Although industrial contaminations vary (Manivasakam, 2016), for experimental purposes this range would be reasonably broad to indicate the fungus' minimum inhibiting concentrations (MIC) for the different pollutants.

3.1.2 Inoculating the fungi

As per manufacturer instructions, 39 g PDA was mixed with one litre of distilled water and autoclaved at 121°C for 15 min before distributing the hot liquid to 100 mm plates, up

to a depth of 5 mm, resulting in approximately 39.3 mL of PDA in each plate. Spores were collected from the innoculated sample by scraping the top of the mold with a sterilized blade and depositing the spores into 5 mL of distilled water. This spore-infused water was then used to inoculate the PDA plates by evenly distributing the water between five plates, and allowing them to incubate at 35 °C for five days until a thick mat of black spores had formed on the plate. This was then used as a spore bank for metal tolerance tests and to cryogenically freeze spores for further studies. To prepare plates for Pb(II) tolerance tests, 1 mL sterile water was added to a PDA plate with healthy spore growth, swirled around to collect spores, and then transferred to 9 mL sterile water so that a ten times dilution is achieved. The spore-infused serum had a dark murky colour, typical of water containing copious amounts of black *A. niger* type spores, although unfortunately spore enumeration could not be done due to lack of suitable equipment. 0.5mL of the spore-infused water was added to each set PDA plate, and agitated to distribute the spores.

3.1.3 Agar well diffusion method

To test which metals the fungus is resistant to, the agar well diffusion (AWD) method was selected (figure 3.1). This quick, easy and cost-effective (M Kumar et al., 2000) method is a good way to gauge a microorganism's minimum inhibitory concentration (MIC). In other words, how much of a specific metal the fungus tolerate before it can't grow anymore? The AWD method entails evenly inoculating the surface of set agar plates (in this instance PDA was used), drilling a 5mm diameter well in the center using a sterilized glass tube, and then introducing a toxin to that well. The toxin would then diffuse radially outwards through the agar with low concentrations around the edges and higher concentrations in the center. Measuring the distance from the center to the edge of the growth would give one an MIC estimate (Chalad et al., 2018). 1.598 g of $Pb(NO_3)_2$ was weighed and dissolved in 100 mL of distilled water. This was then serially diluted until a final Pb(II) ion concentration of 2 000 ppm stock solution was obtained. For the AWD method, 0.5 mL of this Pb(II) stock solution was deposited in the middle of a PDA plate so that each plate contained 1 mg of Pb(II) ions. The plate was again incubated at 35 °C for five days, after which photos were taken. The same approach was taken for all the other metals.

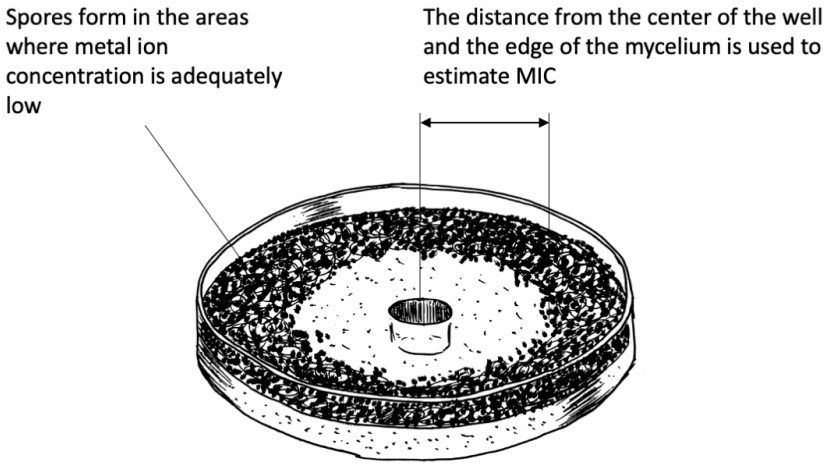

Figure 3.1: A representation of the agar well diffusion method. The concentration decreases towards the edges of the plate, and the fungus can only grow where the concentration is sufficiently low.

3.2 Results and discussion

After incubation, there was spore growth on all the plates, except Cd(II). On this plate a white mat was observed (figure 3.2a). To establish the nature of the white mat, and ensure that it is indeed mycelium, a sample was observed under 40 x microscopic magnification where characteristic mycelial hyphae (Yates et al., 2016) are visible (figure 3.2b). There are numerous explanations for this observation: Either the hostile environment has a spore-suppressant effect on the fungi whereby resources are not allocated to propagation but rather to maintenance; or a genetic mutation occurred whereby the dominant fungal growth does not have the ability to produce spores. The last case would be particularly interesting because there are several benefits to non-propagating fungi, such as human safety from *Aspergillus* respiratory infection (Shah et al., 2004), as well as biological containment in industry. To establish whether this is the case, subsequent experiments would require propagating clones from this plate and observing the fungal behaviour in the absence of heavy metals.

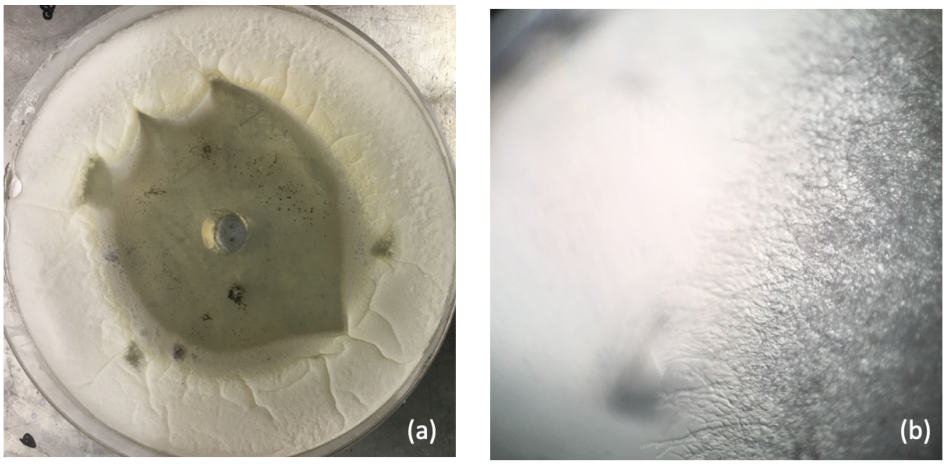

Figure 3.2: (a) Cadmium suppresses mycelium growth up to 23 mm from the centre where 1 mg metal was deposited, (b) White mycelial hyphae on Cd (II) plate at 40 x magnification

In estimating the growth threshold in Cd(II), twelve distance measurements were taken from the edge of the well to the start of the mycelium and an arithmetic mean of the measurements of 23 mm was obtained. Using the solution of the partial differential equation (3.1), and describing free diffusion in one dimension (equation 3.2), (Bonev et al., 2008) an MIC of 875 ppm Cd(II) was estimated.

$$c(x,t) = x(0,0)exp(-\frac{x^2}{4Dt}) \tag{3.1}$$

$$D\frac{\delta^2 c(x,t)}{\delta x^2} = \frac{\delta c(x,t)}{\delta t} \tag{3.2}$$

Where $c(x,t)$ describes the metal concentration as a function of distance from the source and time, x is the distance from the edge of the well, D is the diffusion coefficient of the metal ion, and t is the time of metal ion diffusion.

Other interesting observations were made for Pb(II), Mn(II), Se(IV) and Zn(II), (figure 3.3a), where there was either clearly uninhabitable areas, or a change in spore texture. Only selenium (IV) proved to have areas that are completely hostile for the fungi, with little or no growth in the center (figure 3.3b). In subsequent experiments it may be useful to increase the metal concentration by at least a factor of 10 in all the metals so that clear thresholds can be established.

Another observation is the difference between spore growth close to the well and on the edges. Although denser, the spores around the sides do not appear to be as vibrant and vividly black as the ones in the center. Zinc (II), for example (figure 3.3b), shows a clear deviation from normal spore growth. At a first glance an incorrect assumption was made — that the center ring may simply be covered with a layer of spores that became airborne, thus accounting for the change in texture.

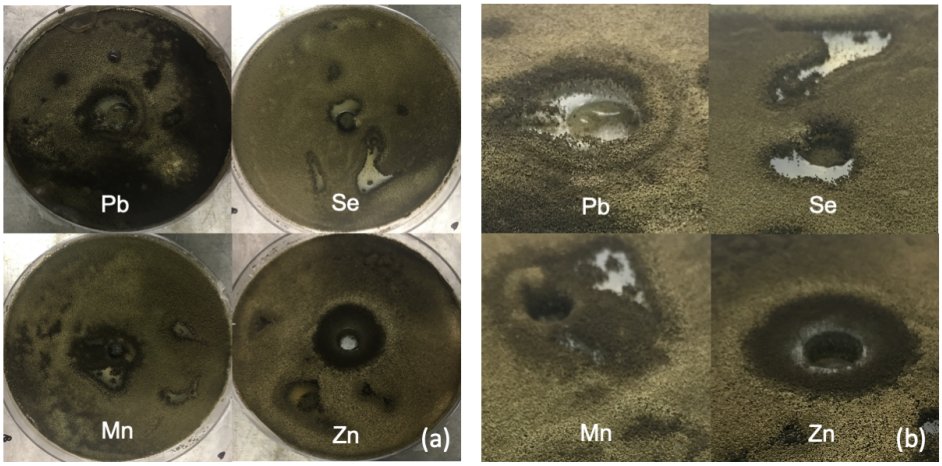

Figure 3.3: (a) Fungal spore inhibition demonstarated in Pb(II), Se(IV), Mn (IV) and Zn(II), (b) Se(IV) closeup shows areas where the metal concentration was too high for the fungi to survive, while Pb(II), Mn(IV) and Zn(II) exhibit a ring around the center

However, upon microscopic inspection, it became clear that at 30 mm from the hole the spores have a very different texture, with numerous empty and collapsed conidiophores which would imply that the spores have already drifted off and that that area was populated earlier (figure 3.4a), whereas there are healthy conidiophores and spore clusters present (figure 3.4b) directly adjacent from the center.

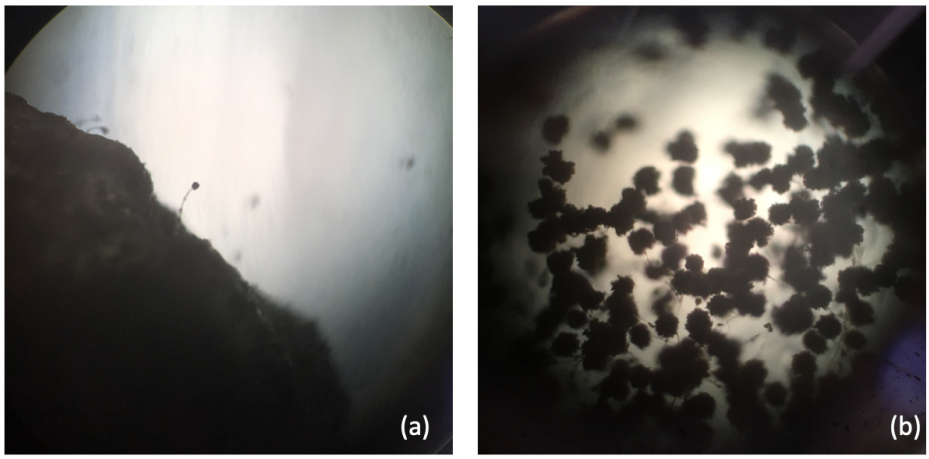

Figure 3.4: (a) Older spores on Zn (II) plate 30 mm from centre, (b): New spores on Zn (II) plate 8 mm from center.

The rest of the plates showed no obvious evidence that the fungus had reached its maximum concentration threshold (figure 3.5), although higher concentrations of these metals could result in the emergence of a clear threshold.

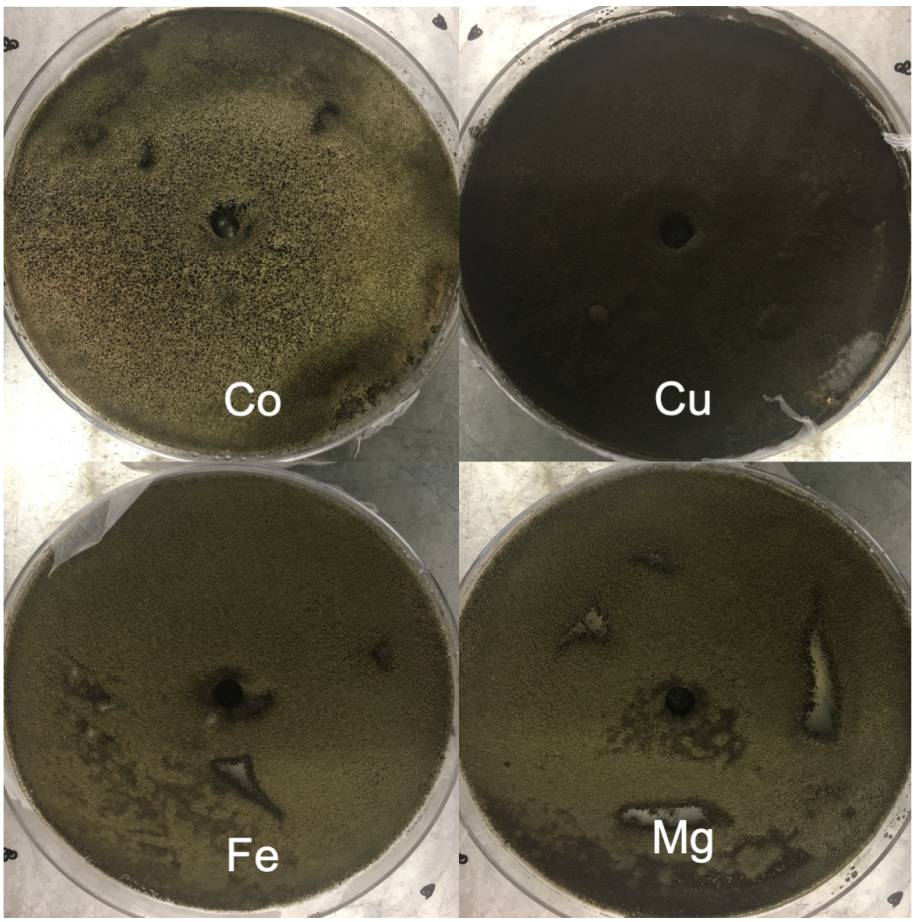

Figure 3.5: Metal solution plates after five days: Little visual evidence that metal tolerance threshold has been reached

Chapter 4:
Finding Optimal Growth and Adsorption Conditions

The aim of this chapter was twofold: to find optimal conditions under which *Aspergillus piperis* can be propagated; as well as optimal conditions under which adsorption can take place. Factors considered were initial Pb(II) concentration, initial solution pH, temperature, and biomass treatment. Parts of this section was published in the journal *Sustainability* in November 2021 (de Wet and Brink, 2021b), as well as Chapter 18: Fungi in the Bioremediation of Toxic Effluents (de Wet and Brink, 2021a) with co-author Dr. H.G. Brink.

4.1 Materials and Methods

4.1.1 Reagents used

All chemicals are manufactured by Sigma Aldrich unless otherwise stated. Potato dextrose agar (PDA) was prepared per manufacturer instructions while a tryptic soy broth (TSB) was made using 10 g L^{-1} vegetable peptone, 10 g L^{-1} D(-)-glucose, 2.5 g L^{-1} NaCl , and 1.25 g L^{-1} K_2HPO_4, autoclaved and allowed to cool.

Pb(II) stock solution was prepared by dissolving 799.2 mg $Pb(NO_3)_2$ in half a litre of distilled water to create 1000 mg L^{-1} stock solution. The stock solution Pb(II) ion concentration was confirmed using a Perkin Elmer AA400 atomic absorbance spectrophotometer (AA) (Perkin Elmer, Waltham, Massachusetts).

The results of the AA were interpreted using equation 4.1:

$$Q_{\mathrm{e}} = \frac{(C_0 - C_{\mathrm{f}})V}{1000W} \tag{4.1}$$

Where Q_e refers to the amount of Pb(II) ions adsorbed by the biomass in mg g^{-1}, C_0 and C_f are the initial and final Pb(II) ion concentrations in mg L^{-1}, V refers to the solution volume in litres, and W is the biomass weight in grams. The experimental conditions resulting in the highest adsorption were selected for further runs.

4.1.2 Optimising biomass growth

4.1.2.1 Agar plate experiments

Before starting, a fungal specimen was sent to Inqaba Biotechnical Industries (Pty) Ltd for DNA extraction, PCR amplification, and sequencing to confirm the species. By isolating the calmodulin gene a positive identification of *A. piperis* was made.

To establish ideal growth conditions, the isolated fungus was plated and inoculated to create a spore stock solution as described in section 3.1.2. The minimum inhibitory concentration from previous experiments (de Wet, Brink, and Horstmann, 2020) informed the Pb(II) concentration ranges selected, thus triplicate PDA plates with varying Pb(II) and pH ranges, as well as three control plates with PDA (already at a pH of 5.6 and with no Pb(II)), were prepared. For the acidic media, 0.1 M HNO_3 was added to 100 mL PDA in volumes of 0.01, 0.1 and 1 mL to create a pH of 5, 4, and 3 respectively. They were then shaken vigorously before being distributed to plates. The solution pH was measured using an Ohaus Starter3000 pH and temperature probe just before the PDA had cooled down enough to solidify. Similarly the 1000 mg L^{-1} $Pb(NO_3)_2$ stock solution was administered to another batch of 100 mL PDA flasks in volumes of 0.5, 1, and 2.5 mL to create Pb(II) concentrations of 50, 100, and 250 mg L^{-1} respectively. 2 mL Pb(II)-infused PDA was retained and diluted 100 times in distilled water before it could set so that the samples could be analysed using the AA to confirm the Pb(II) concentration. An example of what this looks like on an agar plate can be seen in figure 4.1.

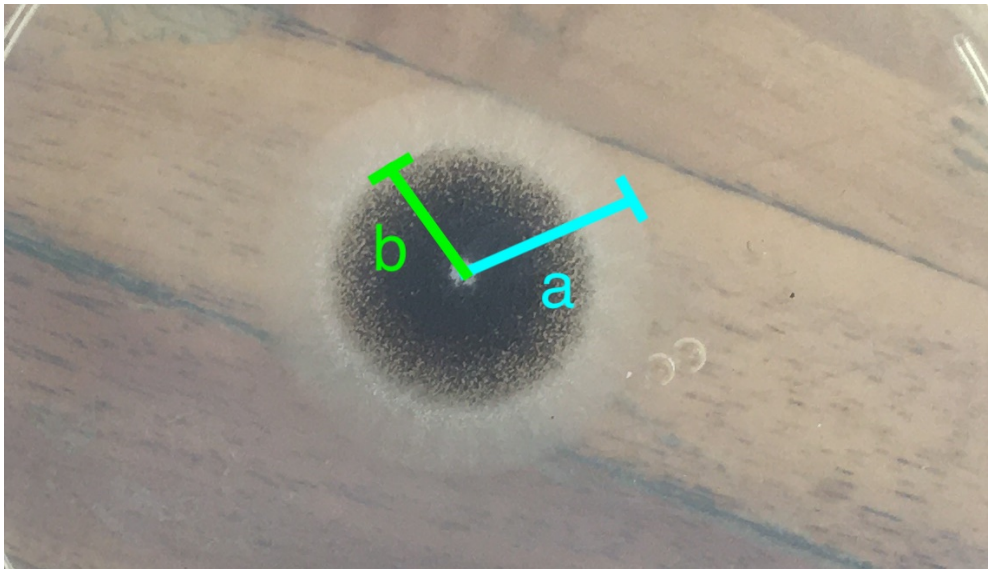

Figure 4.1: An example of *A. piperis* on an agar plate with a pH of 3 after two days. The mycelium grows radially outwards can can be measured from the inoculation point to the edge of the white mycelium (line a), followed by black spore formation soon thereafter (line b).

Once the PDA had solidified, a 0.1 mL pipette tip was used to transfer a 0.2 mm diameter circle of spores to the center of each plate. The plates were then incubated at 35 °C and the distance from the center, where the spores appear as a minute black dot, to the edge of the mycelium was measured every 24 hours to get radial growth estimates. All plates,

including controls, were produced in triplicates.

4.1.2.2 Submerged fermentation experiments

Fungi, like humans, require aerobic respiration to survive and even though *A. niger* species tend to be xerophiles (not requiring a lot of water to grow), a submerged fermentation (SmF) method is selected to test its Pb(II) remediation potential. SmF refers to the process of submerging a culture into a free-flowing liquid substrate (Gupta, 2016) and then agitating the reactor so that aerobic conditions are maintained. This technique is widely utilised in industry because it allows for much more control over mixing, pH, nutrients, and product analysis than solid state fermentation (SSF), thus most large-scale enzyme production in industry makes use of SmF, including processes involving *A. niger* (Pandey et al., 2019).

There are four main approaches to SmF: Batch culture, where the liquid substrate, inoculation and other compounds are added at the beginning of the run and left as-is to incubate; fed batch culture, where nutrients such as glucose gets periodically or continuously added to the reactor once they become depleted; perfusion batch culture, where the medium is circulated so that new medium is constantly available; and continuous culture, where new medium is added to the reactor with an increasing nutrient profile that reflects the growing biomass demands (Brahmachari and Demain, 2017, p. 21). Batch fermentation was the most applicable for this study so that nutrient depletion and any other profile changes in the medium could be measured.

As a liquid substrate, tryptic soy broth (TSB) was selected. While hot, the TSB was distributed amongst 100 mL autoclaved reactors and left to cool to room temperature inside a sterile environment. Inoculation was done by adding 0.5 mL spore solution (the same method as with plating) to each reactor, which took place inside a sterile positive displacement chamber. To study the effects of pH, Pb(II), and growth medium, 1 mL of spore solution was used to inoculate 100 mL bioreactors containing TSB in batches of six reactors. The reactors were incubated at 35 °C and 135 rpm for three days. The mycelium was then drained, rinsed with distilled water, and dried for four hours at 60 °C before being weighed.

4.1.3 Optimising adsorption: Using growing mycelium

To test whether the fungus has any capacity for Pb adsorption, it was grown in the presence of Pb and the medium Pb concentration was tested before and at various intervals during this process. This would theoretically give the fungus the greatest capacity for adsorption because it develops in the hostile environment and has the opportunity to adapt to it.

4.1.3.1 Submerged fermentation experiments

Submerged fermentation was again used, as described above, however this time the objective of the experiments was to see whether adsorption takes place during mycelial growth. This time, 3, 4, and 5 mL of the inoculated TSB was removed from each reactor and replaced with autoclaved Pb(II) stock solution (10 000 ppm) of the same amounts. This meant that the reactors had final values of 300, 400, and 500 ppm of Pb(II), as well as a

control sample that contained no Pb(II). Finally a sterilised ball of cottonwood was used to plug the top of the Erlenmeyer flask reactors so that aerobic respiration could take place in axenic (only one controlled species is present) conditions (figure 4.2).

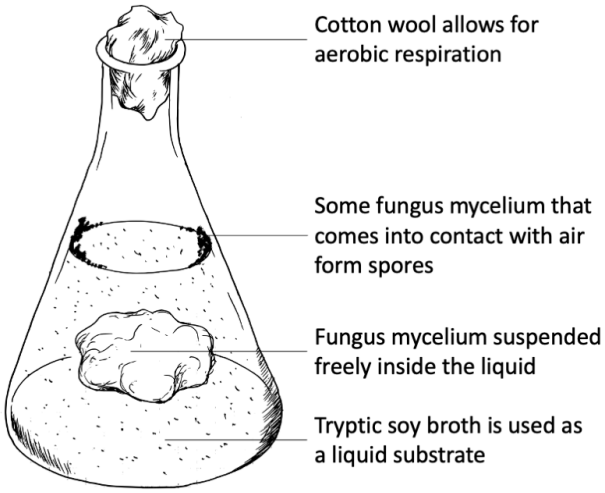

Figure 4.2: An illustrated example of a submerged fermentation reactor.

4.1.3.2 Sacrificial samples

Sacrificial sampling is a simple method to estimate intermittent progress inside a single reactor (Filler et al., 2008) . A large set of reactors are prepared and incubated identically. Reactors are then "sacrificed" one by one at predetermined time-intervals for analysis. This is an especially useful technique to determine a property which would require the organism to be destroyed, such as measuring biomass. Although it is impossible to replicate the exact reactor conditions every time, these measurements represent a good estimation of the progress occurring inside a single reactor.

For this study, eight 100 mL reactors were inoculated as described above, prepared to have a concentration of 500 ppm Pb(II), and incubated at 35 °C on a 120 rpm shaker for four days. Every 12 h a 2 mL sample was taken from reactor 8 as a control to measure the Pb(II) ions using atomic absorption spectroscopy (AA) and one other reactor was sacrificed. Each sacrificial reactor was filtered so that pH, glucose, and Pb(II) concentration could be measured while filter paper containing the mycelium was dried over a period of 12 hours and weighed to measure the mycelium biomass.

4.1.4 Optimising adsorption: Using dried biomass

To study the adsorption profile of the mycelium in more depth, mycelium was removed from the fermentation conditions and dried out. By eliminating factors such as small variations in fermentation medium and conditions, and being able to quantify the biomass precisely beforehand, more accurate adsorption-specific results can be obtained by essentially utilising dead instead of living biomass for adsorption.

It must be noted however that despite the harsh processes that the fungus underwent, given opportunity it would consistently reanimate and start growing again. This was

most evident when a Brunauer–Emmett–Teller (BET) analysis was attempted, and during sample processing the fungus (or at least some of its cells) not only survived being heated to 80°C, but started growing in a vacuum. If left for long enough in nothing but a solution of purified water and lead nitrate, the surviving cells would feed off the dead ones and visible mycelial growth would quickly be present in the reactor. The fungus proved to be exceptionally hardy and prolific, which was mostly useful for this study, but also a nightmare for peers who shared the laboratory space.

4.1.4.1 Propagating wet and dry biomass for adsorption studies

For adsorption studies, enough of the biomass (mycelium) needed to be propagated for several experimental runs. To do so, ten 100 mL Erlenmeyer flasks were inoculated and incubated for three days as described above producing on average 4.45 g wet mycelium, or 0.0907 g dry mycelium per 100 mL bioreactor. This averaged out at roughly 1 g dry biomass per litre of tryptic soy broth (TSB). The wet mycelium was then adsorbed from solution using a tea sieve and rinsed with distilled water. Thereafter the mycelium was either used immediately, or dried in an oven at 60 °C for four hours.

To compare mycelium grown in the presence and absence of Pb(II), the same method was used to create Pb(II) bioreactors, however 5 mL of 1000 mg L^{-1} Pb(II) nitrate stock solution was added to create a 50 mg L^{-1} Pb(II) medium. After incubation the mycelium was washed and placed in 0.1 M HNO_3 for three hours to remove any Pb(II) sequestered by the mycelium. Thereafter the mycelium was once again washed and dried.

0.1 g dried mycelium was then added to 50 mL prepared solution in 100 mL vials. With a constant biomass of 10 g L^{-1} (dry), the solution Pb(II) concentration, temperature, and pH varied according to the experimental design. The samples were then incubated at 100 rpm for two hours in a submerged shaker and then centrifuged to remove the biomass while the supernatant was passed through a 0.45 μm filter and kept for AA analysis.

4.1.4.2 Optimising adsorption conditions: Fractional factorial experimental design

The purpose of this experimental design is to optimize the average response value (% Pb(II) removal) and minimise effects of random variability which is present in most processes (Lochner and Matar, 1990). Procedures like one factor at a time neglects factor interactions such as the combined effects of pH and temperature on Pb(II) adsorption. An alternative approach is to consider all combinations of factors at various levels. Factors studied here are: Pb(II) ion concentration, temperature, pH, and biomass preparation. Each factor has a particular set of levels, or variable values such as a pH of 2, 3, or 4. Attempting to combine all factors at all levels would lead to an exponential amount of samples. For example, to test all interactions between all four factors, each with three levels, would require $3^4 = 81$ trials per experimental run, moreso if the trials are to be done in triplicates. Limiting levels to two at a time (such as only considering a pH of 2 and 3) significantly reduces the number of trials ($2^3 = 8$) and allows for finding optimal conditions using an iterative approach and then applying statistical analysis to assess which factors had the largest effect on the response value and estimate how the factors interacted with each other.

Using a two-level fractional factorial design approach (Lochner and Matar, 1990), the runs were broken up into two sets of trials, allowing for all four factor interactions to be explored at four levels and requiring only 16 trials. The 16 trials were broken up into two blocks of eight trials, each of which were done in triplicates. Along with the control samples, each experimental block thus had 27 trials. After every run statistical analysis was applied to the results to determine the level values for the subsequent run. Each trial has a unique combination of levels for each factor, and when the difference between level averages for each factor is calculated, the highest-scoring factors or factor interactions will be the ones with the strongest effect on Pb(II) adsorption. This way the experimental results will quickly converge to an optimised combination of pH, temperature, Pb(II) concentration, and biomass preparation for maximum adsorption.

The level selection was carefully considered: If the range is too wide, much more iteration is required and if the range is too narrow an optimal level may be missed. The selected starting level for Pb(II) concentration was based on reasonable expectations drawn from the fungal studies referred to earlier, while the pH and temperature values were selected based on practical considerations such as the fungal thermal threshold and Pb(II) solubility limits. pH was expected to play a large role in the adsorption as it can affect the metal speciation, sequestration, or mobility. The maximum pH considered was 5 to avoid precipitation effects from Pb(II) hydrolysis which is expected to occur at a pH of around 6.3 for $Pb(NO_3)_2$.

To control for variability in biomass water retention, all biomass used in adsorption were dried and preparation fell into two categories: Mycelium grown in the absence of Pb(II), and that grown in 50 mg L^{-1} Pb(II) ions, and then submerged in 500 mL 0.1 M nitric acid to remove the Pb(II) from the active sites. The hypothesis was that biomass grown in the presence of Pb(II) could express specific adsorption sites/surface characteristics with elevated Pb(II) removal characteristics as a defense mechanism. Table 4.1 displays the levels for the initial run, and based on the outcome thereof, levels for subsequent runs were selected to gain more resolution.

Table 4.1: Starting level values for factors: Pb(II), pH, temperature, and biomass

Factor	Level 1	Level 2	Level 3	Level 4
Pb(II) (mg/sample)	1	3	6	8
Solution pH	5	4	3	2
Temperature (C°)	25	30	35	40
Biomass preparation	No Pb	Pb	No Pb	Pb

4.1.4.3 Desorption and regeneration studies

To see whether it was possible to regenerate the mycelium, post-adsorbed biomass was added to a 500 mL solution of 0.1 M HNO_3, left for 3 hours, and centrifuged after which the HNO_3 was analysed using AA.

4.2 Results and discussion

4.2.1 Optimising biomass growth

4.2.1.1 Agar plate experiments

The results for the potato dextrose agar (PDA) plates can be seen in figure 4.3.

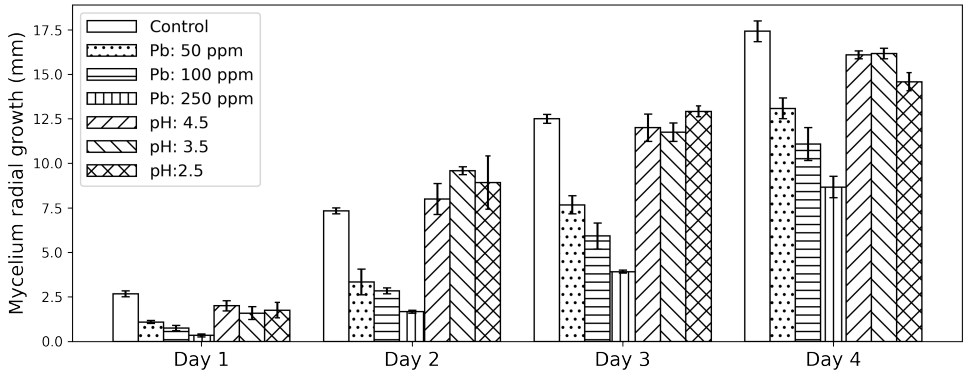

Figure 4.3: Potato dextrose agar plate study for optimisation of growth conditions: Observing the effects of Pb(II) and pH by measuring radial growth.

As with most fungi (de Wet and Brink, 2021a), *A. piperis* showed good growth at the control pH of 5.6, and by the second day the fungus showed good growth even on a much more acidic medium. While the low pH growth is slightly more stunted than the control group, this property may prove useful for industrial, less controlled applications because it not only buffers against bacterial infection, but Pb(II)-contaminated water is often at a lower pH. Initial Pb(II) concentration seems to have the largest effect on the mycelium growth at the beginning, where the fungus only achieves 40.6%, 28.1%, and 12.5% of the control growth for 50, 100, and 250 mg L^{-1} respectively. However this steadily increases and by day four the radial growth for the Pb(II) plates have reached 75.1%, 63.6%, and 49.8% of the control growth. This could imply that the fungus is initially inhibited by the Pb(II) but manufactures a means of coping with the toxic environment.

4.2.1.2 Submerged fermentation experiments

The submerged fermentation for optimal biomass growth experiments yielded unclear results. Despite the studies being undertaken in sextuplicates, a large variation of biomass yield still occurred within identical experimental conditions. Surprisingly neither a pH of 7, 5, and 3, nor Pb(II) concentrations of 50, 100, and 250 consistently resulted in significant yield differences. In fact biomass yield was often much higher in the presence of Pb(II) than in the control group, but not consistently so.

However the factors that had a consistent impact on biomass yield was spore inoculation and to a lesser extent growth medium. For the 100 mL reactors, the average spore inoculation to biomass ratio (measured in mL spore solution per gram dried biomass after 3 days) were as follows: 3.33, 14.3, and 35.7. Because *A. piperis* is, like most mold,

such a prolific spore producer, increasing inoculation concentration is much more feasible than increasing incubation times for the reactors.

Thus mass production of the biomass can be undertaken in a variety of conditions without significant inhibition from Pb(II) or pH, and provided that there are ample nutrients available with 50 mL spore solution per litre of medium, a yield of at least 1 gram dry biomass per litre of medium can be harvested.

4.2.2 Optimising adsorption: Using growing mycelium

4.2.2.1 Submerged fermentation experiments

In all the runs, the TSB started out opaque, and became clearer as mycelial growth commenced. Mycelial growth stagnated and stopped after about five days, presumably when the nutrients were depleted. Around day three a thick mat of black spores rapidly formed at the surface of the broth where mycelium came into contact with air (figure 4.4a). The drained mycelium (figure 4.4b) had an amorphous consistency, and retained a lot of moisture. The mycelium appeared uniform in texture, colour and consistency. Mycelium that was inadvertently exposed to air took on a whiter, opaquer colour, and had a more leathery texture.

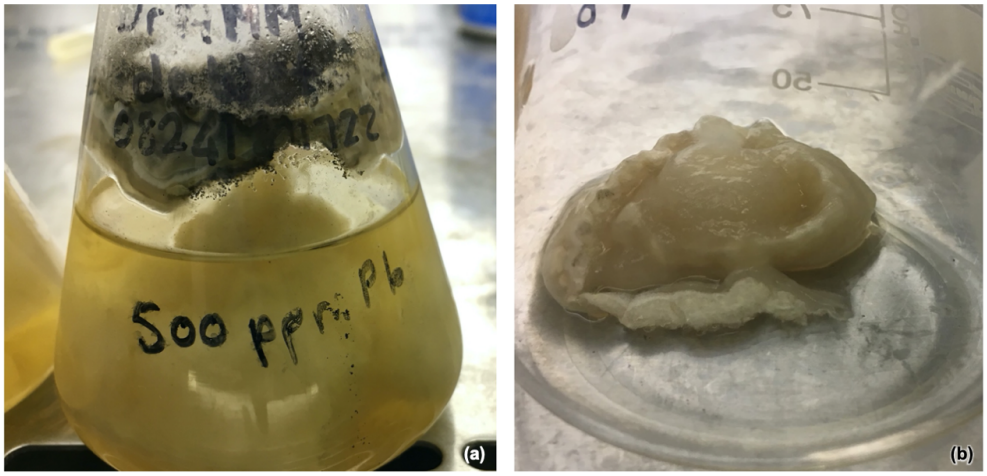

Figure 4.4: (a) Spores formed after three days where the mycelium came into contact with air, (b) Drained mycelium from a sacrificial sample after four days

One 2 mL sample was taken from each reactor and analysed using AA. The results indicated that Pb(II) was reduced to different extents in all three reactors (figure 4.5). Small upward surges in concentration that all reactors exhibited at some point appear to have no specific timing and may be due to measurement errors. After five days the biggest drop in concentration was that of reactor 2 with a 68.3 % decrease in Pb(II). It is important to note that the initial concentrations of the reactors did not reflect the intended Pb(II) concentrations. In each case the measured concentration was slightly lower than expected, with 282, 375, and 407 ppm instead of 300, 400, and 500 ppm. To check whether some of the Pb(II) was precipitating out of solution, two uninoculated reactors were prepared with 300 ppm Pb(II) and four samples were taken from each reactor over a two day period. One reactor was left on a table top while the other was placed on the same shaker where

the reactors were incubated. The reactor on the table top had at most an 8 % decrease in Pb(II), although the concentration fluctuated with each measurement and the Pb(II) concentration in the agitated reactor on the stirrer actually increased from the starting concentration by 2 % which can be attributed to measurement error during the serial dilution preparation for AA analysis. When compared to the consistent decrease in Pb(II) in the other runs, neither of these control results appear to indicate that precipitation is the primary driver behind the sustained drop in metal ions observed in other runs. Rather, measurement errors and possibly a small amount of initial precipitation would account for the deviations.

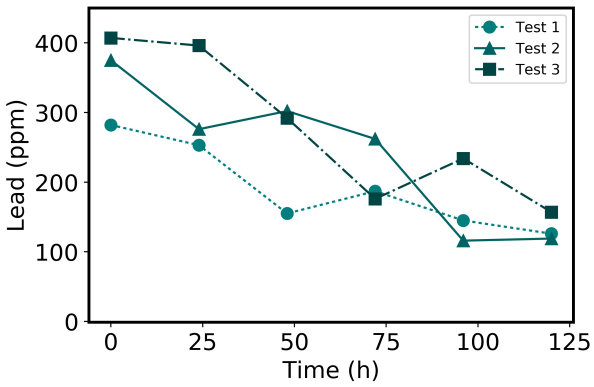

Figure 4.5: Pb(II) reduction in early trials with an average of 61.7 % reduction across the three reactors

4.2.2.2 Sacrificial samples

Pb(II) AA values for the sacrificial samples were much closer to the desired starting values at 499.5 ppm for the first sacrificial reactor and 489.8 ppm for the control. The average Pb(II) values were calculated using the arithmetic mean of the sacrificial samples and the control reactor and do not deviate meaningfully from each other (figure 4.6a), which could indicate that the sacrificial samples are a fair representative of what would happen in a hypothetical single reactor. The final average Pb(II) value was 86.0 ppm, an 82.6 % decrease from the starting value.

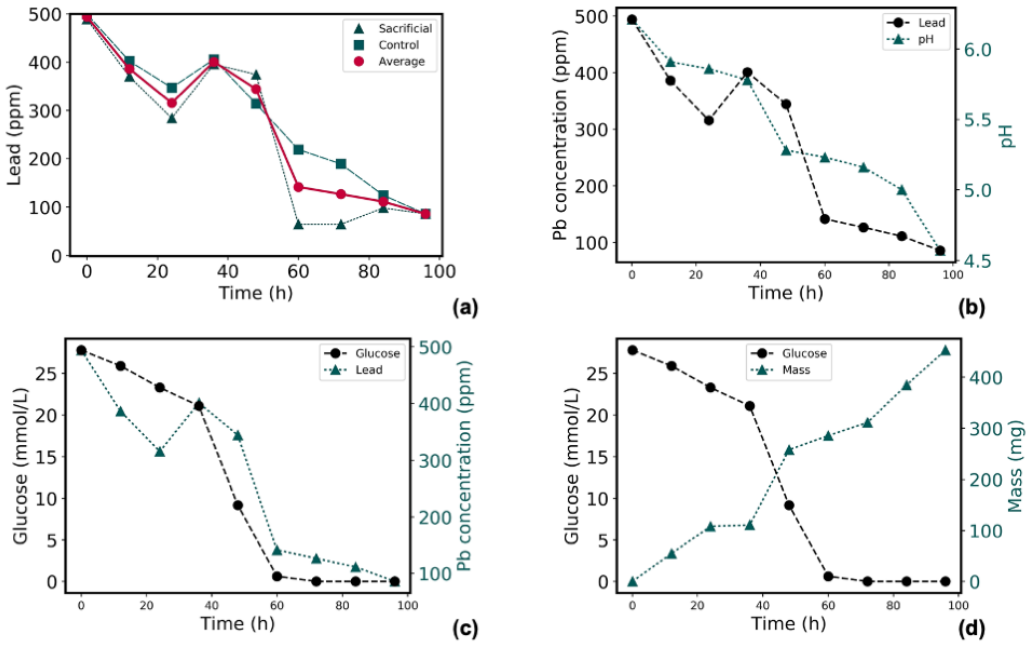

Figure 4.6: (a) The Pb(II) values from the sacrificial samples and the control follow a similar trend, (b) Pb(II) and pH are reduced at a similar rate, (c) Glucose depletion compared to Pb(II) remediation, (d) Glucose depletion compared to mycelium mass increase

Pb(II) and pH both decreased at a similar rate (figure 4.6b) which means that pH measurements could potentially be an inexpensive, continuous way to roughly monitor remediation progress in industry, instead of relying on expensive and cumbersome AA analysis. pH dropped from 6.21 to 4.57, a 26.4 % decrease.

The mechanism whereby *A. piperis* removes the Pb was still unknown at this stage, but it was suspected that biosorption may be the primary driving force for two reasons: *A. niger* has been reported to utilize biosorption for remediation, and the drop in pH would exclude many alternative mechanisms.

By comparing the average Pb concentrations, it seemed as though the maximum remedial potential is achieved after 2.5 days, around the time when glucose becomes completely depleted (figure 4.6c) from an initial value of 27.8 mmol L^{-1}. This is also the time when the fungi goes into a state of spore-creation. A black mass of spores suddenly became visible on the TSB surface around this time, presumably because the lack of glucose triggers a propagation reaction. On the other hand, when comparing glucose levels to an increase in biomass (figure 4.6d), there seems to be little growth stagnation despite the nutrient deficiency. The growth rate decreases slightly as glucose depletes and then suddenly goes through a period of accelerated growth, presumably as it undergoes a metabolic shift, with a final mycelial mass of 453.0 mg.

4.2.3 Optimising adsorption: Using dried biomass

4.2.3.1 Optimising adsorption conditions

The results of the adsorption experiments can be seen in figure 4.7, with the variable levels for reactors 1 to 16 in table 4.2 and 4.3. The sample with the highest Pb(II) adsorption

was sample 5 with an equilibrium Pb(II) adsorption of 87.34%. This sample had an initial Pb(II) concentration of 200 mg L^{-1}, initial pH of 5, a constant temperature of 25°, and biomass that was not grown in the presence of Pb(II).

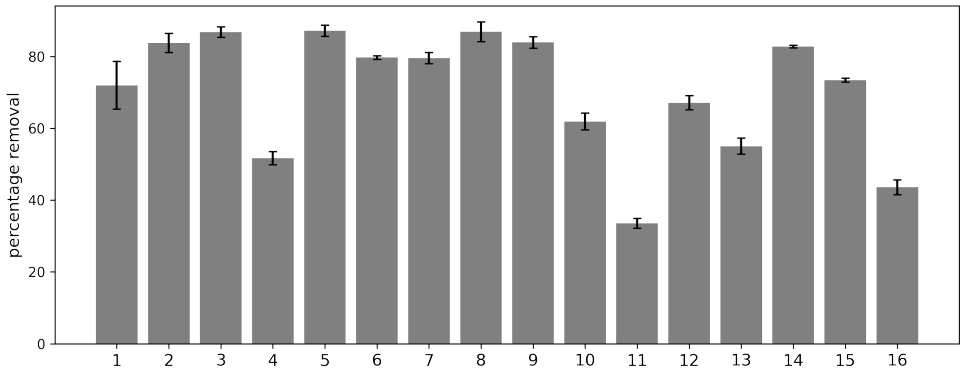

Figure 4.7: Average % Pb(II) ion adsorption for reactors 1 to 16.

Table 4.2: Sample variable conditions for Set A: Reactors 1 - 8

Sample	1	2	3	4	5	6	7	8
Pb (ppm)	100	100	100	100	200	200	200	200
pH	5	5	4	4	5	5	4	4
T (C°)	25	30	25	30	25	30	25	30
Pre-treat	Pb	ctrl	ctrl	Pb	ctrl	Pb	Pb	ctrl

Table 4.3: Sample variable conditions for Set B: Reactors 9 - 16.

Sample	9	10	11	12	13	14	15	16
Pb (ppm)	300	300	300	300	400	400	400	400
pH	3	3	2	2	3	3	2	2
T (C°)	35	40	35	40	35	40	35	40
Pre-treat	ctrl	Pb	Pb	ctrl	Pb	ctrl	ctrl	Pb

Interaction effects from the different variable levels are shown in figure 4.8. These results suggest that the most prominent factor that affects the Pb(II) adsorption success is the pretreatment of the biomass, with exposure to Pb(II) ions followed by nitric acid treatment having a poor outcome on adsorption.

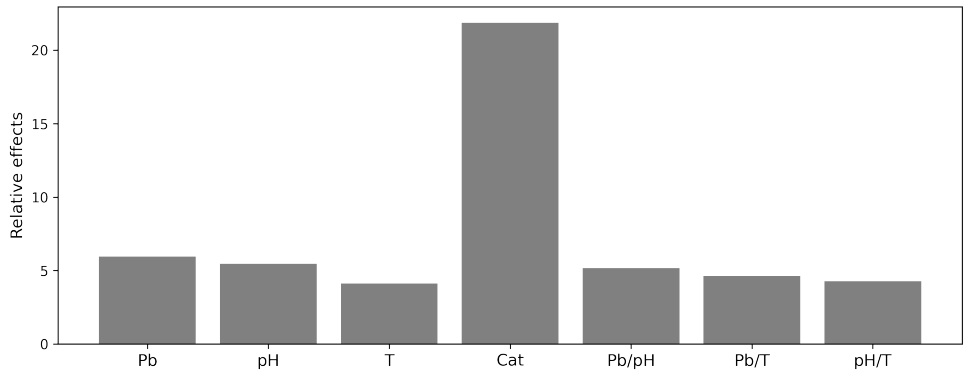

Figure 4.8: Relative effects of variable levels and their interactions: Biomass pre-processing has the most prominent effect on adsorption capacity.

Pb(II) adsorption percentage (figure 4.9a) across a pH of 2 - 5 had a very small standard error of the mean of 2.64%, with the lowest adsorption taking place at an initial pH of 2 (76.4% adsorption), and the highest at 4 (87.8 %). This suggests that optimal initial pH for adsorption should be in the rage of 3 - 5 rather than below 3, although fungal survival and adsorption capacity is not markedly inhibited by starting pH. The measured effect of temperature on Pb(II) (figure 4.9b) adsorption had a nearly insignificant standard error of the mean of just 1.46% adsorption, with no strong evidence that temperature affects the equilibrium adsorption.

On average, using untreated biomass (in other words grown in TSB in the absence of Pb(II)) resulted in an 11.04% greater Pb(II) removal. This was confirmed in a separate experiment by keeping all other factors the same and only changing the biomass type, which resulted in a 61.15 % removal for the untreated biomass, and a 16.02 % removal for the Pb(II) treated biomass from an initial concentration of 182.2 mg L^{-1}, confirming that Pb(II) biomass treatment greatly reduces adsorption capacity. It is likely that this reduction in adsorption capacity was a result of adsorption taking place during the growth phase in Pb(II) spiked medium, which reduced the number of available sites for adsorption by the dried adsorbent.

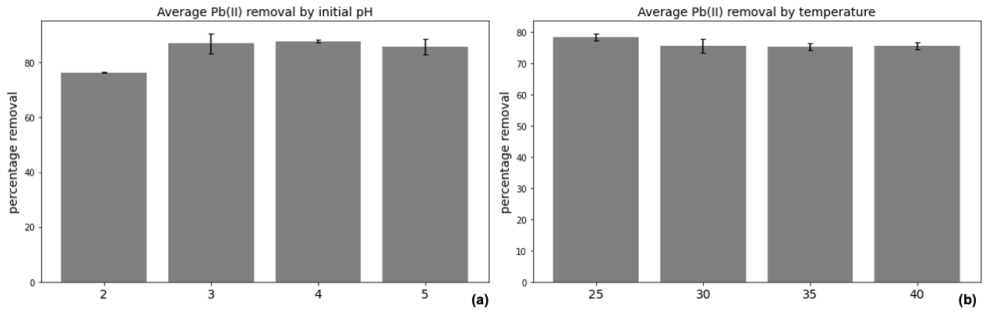

Figure 4.9: Average Pb(II) removal by pH (a) indicates that adsorption is optimal between 3 and 5, and temperature (b) indicates that adsorption isn't significantly affected by temperature.

4.2.3.2 Desorption and regeneration studies

To study the biomass regeneration after adsorption, an initial Pb(II) medium concentration of 6.22 mg L^{-1} was confirmed. After exposing the biomass to one litre of the medium, the concentration had dropped to 3.48 mg L^{-1}, indicating that the biomass retained roughly 2.48 mg of Pb(II) ions. The biomass was then dried and placed in HNO_3 for an hour after which the acid was also tested using the AA. The HNO_3 concentration turned out to be 2.23 mg L^{-1}, which suggests that some of the Pb(II) ions were not completely adsorbed from the biomass, but that desorption in general is possible.

Regeneration however has proved not to be feasible as indicated by the poor performance of Pb(II)-treated biomass. This is likely due to the destruction or occupancy of surface active sites caused by the strong acid, as previously eluded to by Veenhuyzen et al. (2021). In that study $Ca(NO_3)_2$ was used after similarly negative HNO_3 regeneration results were observed, leading to much better regeneration. This will be attempted in future studies.

Chapter 5:
Adsorption Isotherm and Kinetic Studies

The aim of this chapter was to glean information about *Aspergillus piperis'* adsorption capabilities by conducting isotherm and kinetic experiments and then fitting the resulting data to established models. This section is based on an extraction of a manuscript published in the journal *Sustainability* in November 2021 (de Wet and Brink, 2021b) with co-author Dr. H.G. Brink.

5.1 Models and equations used

5.1.1 Isotherm studies

Equilibrium adsorption isotherm experiments were carried out at 30°C over a period of 24 hours for initial concentrations of 100, 500, 1500, and 2000 mg L^{-1}.

5.1.1.1 One and two-surface Langmuir isotherm models

Langmuir isotherm models were considered for this study and using least squares regression, an isotherm was fit to equation 5.1:

$$Q_e = \frac{Q_{max} K_L C_e}{1 + K_L C_e} \tag{5.1}$$

Here $Q_{\max}$ refers to the maximum saturated monolayer adsorption capacity in mg g^{-1}, while K_L is the Langmuir equilibrium constant in L mg^{-1} and C_e is the Pb(II) equilibrium concentration in mg L^{-1}.

Another approach considered is the two-surface Langmuir model, where it is assumed that adsorption takes place on two types of surfaces. Equation 5.2 describes this:

$$Q_e = \frac{Q_{max,1} K_{L,1} C_e}{1 + K_{L,1} C_e} + \frac{Q_{max,2} K_{L,2} C_e}{1 + K_{L,2} C_e} \tag{5.2}$$

Here the two surface type properties are indicated with subscripts.

5.1.1.2 *Freundlich isotherm model*

To study the reversible, non-ideal, multilayer adsorption, the Freundlich isotherm was used, as described in equation 5.3:

$$Q_e = K_F C_e^{\alpha} = K_F C_e^{1/n} \tag{5.3}$$

In this case, K_F is the Freundlich constant with units of (mg/g)(mg/L)$^{-\alpha}$, where adsorption is favourable when $\alpha < 1$, linear when $\alpha = 1$, and unfavourable when $\alpha > 1$.

5.1.2 Kinetic studies

For kinetic studies, all 100 mL reactors with 50 mL solution had a starting Pb(II) concentration of 100 mg L^{-1}, and were tested under three different temperature conditions: 25°C, 30°C, and 35°C. The reactors were placed in a submerged incubator for an hour until they had reached the desired temperature and samples were taken to get an initial concentration for each of the triplicates. 0.1 g biomass was then rapidly added to each reactor and samples were then taken and filtered in 3 minute intervals for the first 10 minutes, and then over longer periods of time (see figure 5.4 for timestamp details). Various kinetic models were then fitted to this data to determine possible rate and mechanisms of adsorption (Largitte and Pasquier, 2016), (Wang and X Guo, 2020).

5.1.2.1 *Empirical models*

While the empirical models do not generally describe any physical properties, they can help describe the rate of adsorption.

Pseudo-first-order (PFO) model

Proposed by Lagergren (Sahoo and Prelot, 2020), this model is usually applicable when the concentration of adsorbate is high relative to the active sites. This scenario typically occurs during the start of the adsorption. The PFO Pb(II) adsorption rate for *Aspergillus* is expected to range from 0.0190 to 0.1676 (Ji et al., 2017). The analytical form of the PFO can be seen in equation 5.4.

$$Q = Q_e(1 - e^{-k_1 t}) \tag{5.4}$$

Where the equilibrium adsorption capacity, Q_e (mg g^{-1}), and the first order rate constant, k_1 (min^{-1}), are solved for different initial concentrations, C_0 (mg L^{-1}).

Two-phase adsorption

The two-phase adsorption model is based on the PFO, but assumes that adsorption takes place in a slow and a fast step.

$$Q = Q_{fast}(1 - e^{-k_{fast} t}) + Q_{slow}(1 - e^{-k_{slow} t}) \tag{5.5}$$

Where Q_e is solved for each C_0, and a global Q_{fast}, Q_{slow}, k_{fast}, and k_{slow} are fitted.

Pseudo-second-order (PSO) model

Proposed by Ho and Forster (1996), this model is often applicable when there is an abundance of active sites in a low concentration of adsorbate. When the adsorbate concentration is low enough the Langmuir kinetic model can be simplified to a PSO model. The PSO Pb(II) adsorption rate for *Aspergillus* is expected to range from 0.0019 - 0.0200 (Ji et al., 2017). The analytical form of the PSO model can be seen in equation 5.6:

$$Q = \frac{k_2 Q_e^2 t}{1 + k_2 Q_e t} \tag{5.6}$$

Where Q_e and the second order rate constant, k_2(g mg^{-1} h^{-1}), are solved for each C_0.

5.1.2.2 External diffusion

The external diffusion models assume that diffusion through the boundary layer in the solution is the rate limiting step. In other words external mass transfer (EMT) plays a bigger role than internal mass transfer (IMT). This relationship can be seen in figure 5.1.

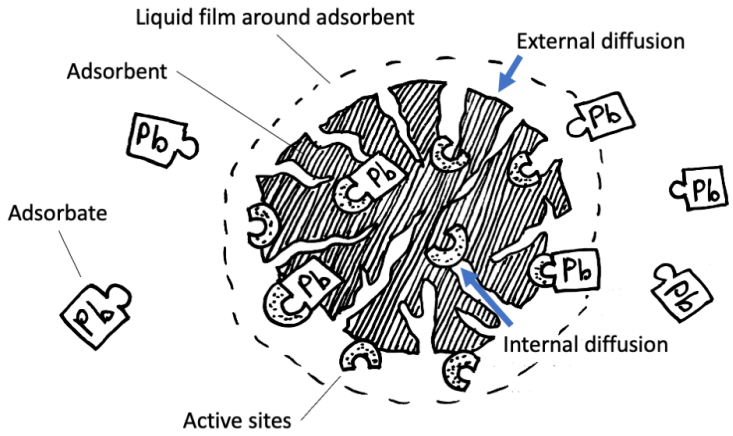

Figure 5.1: The Pb(II) (adsorbate) needs to get to the active sites in the mycelium (adsorbent). Internal and external mass transfer is represented by blue arrows.

Mathews and Weber (M & W) model

$$Q = Q_e(1 - e^{k_{M\&W} S t}) \tag{5.7}$$

Here the $k_{M\&W}S$ term describes the external diffusion, with S the outer surface area per volume of reactor (m^{-1}) and $k_{M\&W}$ in (m s^{-1}).

5.1.2.3 *Internal diffusion*

Internal diffusion models assume that diffusion from the surface and into the adsorbent pores is the rate limiting step.

Crank diffusion model

To quantify this, the EMT model described by Veenhuyzen et al. (2021), which is based on Largitte and Pasquier (2016) as well as Prasad and Srivastava (2009), is used.

$$\frac{\delta C_{\mathrm{B}}}{\delta t} = k_{\mathrm{f}} \frac{a}{V}(C_{\mathrm{B}}) \tag{5.8}$$

$$ln\frac{C_{\mathrm{t}}}{C_0} = -k_{\mathrm{f}} \frac{a}{V} t \tag{5.9}$$

Here C_B refers to the bulk adsorbate concentration, a is the total absorbent area, V is the reactor volume, and k_f is the mass transfer coefficient, which is equal to $k_{M\&W}$, while (a/V) is equal to the the outer surface area per reactor volume, S, both of which can be obtained from the M & W model.

Once inside the mycelium, the adsorbent is modeled as a sphere with radius r according to the Crank model (equation 5.10).

$$\frac{\delta Q}{\delta t} = \frac{D_{\mathrm{e}}}{r^2} \frac{\delta}{\delta r}(\frac{r^2 \delta Q}{\delta r}) \tag{5.10}$$

This can be expressed in equation 5.11, which assumes that the IMT is the limiting rate.

$$\frac{Q}{Q_{\max}} = \frac{6}{\pi^2} \Sigma \frac{1}{n^2} exp(\frac{-D_{\mathrm{e}} n^2 \pi^2 t}{r^2}) \tag{5.11}$$

As this approaches infinity, it's useful to break the equations up according to experimental times (equation 5.12).

$$\frac{Q}{Q_{\max}} = \begin{cases} 6(\frac{D_{\mathrm{e}} t}{R^2})^{1/2}[\pi^{-1/2} - (\frac{1}{2})(\frac{-D_{\mathrm{e}} t}{R^2})^{1/2}], |\frac{Q}{Q_{\max}} < 0.8 \\ 1 - \frac{6}{\pi^2} exp(\frac{D_{\mathrm{e}} \pi^2 t}{R^2}), |\frac{Q}{Q_{\max}} \geq 0.8 \end{cases} \tag{5.12}$$

Once D_e and k_{f} are established, the relative influence of EMT and IMT can be gauged by using the Biot number for mass transfer (equation 5.13). If Bi is larger than 100, the adsorption rate might be limited by IMT, otherwise EMT is the controlling factor.

$$Bi = \frac{k_f d}{D_e} \tag{5.13}$$

5.1.2.4 Adsorption onto active sites

Active site models assume that the rate is limited by the number of active sites on the adsorbent.

Langmuir kinetics model

Unlike the previous models, the Langmuir model represents a reversible reaction where desorption is taken into consideration as well. The nonlinear analytical form can be seen in equation 5.14 (Largitte and Pasquier, 2016).

$$Q = Q_e \frac{k_a}{k_a + k_d}(1 - e^{-(k_a+k_d)t}) \tag{5.14}$$

Where k_a and k_d denote the adsorption and desorption rate coefficients in s^{-1}.

5.2 Results and discussion

5.2.1 Isotherm studies

Before fitting the data to models, the maximum experimental adsorption capacity at 30, 35, 40 and 45 °C was determined. Initial Pb(II) concentrations above 1000 mg L^{-1} result in leveled-out adsorption concentrations (figure 5.2), suggesting that the active sites on the biomass are saturated above these levels. Taking the average of all the datapoints above 1000 mg L^{-1}, the experimental Q_{max} is thus 267.41 ±19.46 mg g^{-1}.

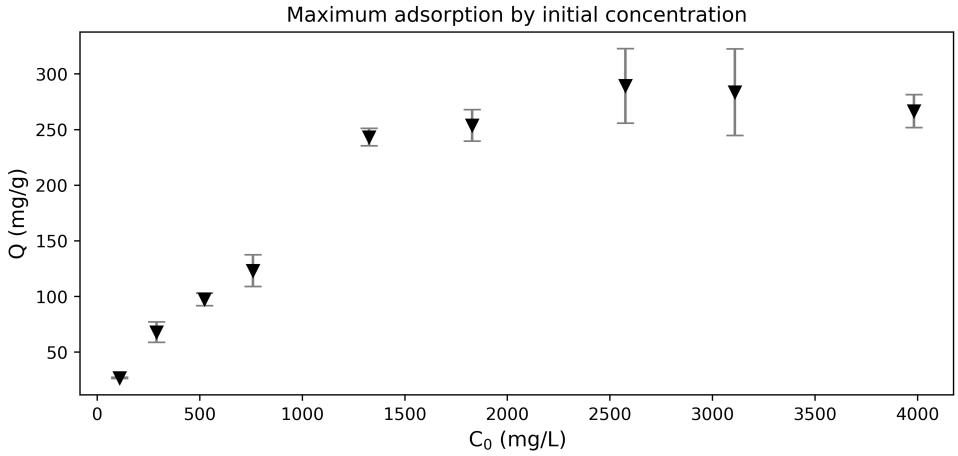

Figure 5.2: Maximum experimental adsorption capacity was determined by taking the average adsorption values above 1000 ppm.

The data used for the isotherm studies contained significant variability at elevated Pb(II) concentrations ($C_0 > 1000$ mg L^{-1}). This is likely due to small variations during serial dilutions for AA measurement and the exponential effect this has on final concentration readings. Because there was no obvious trend between adsorption results at different

temperatures, a one-way ANOVA variance test was done between the datasets for the equilibrium concentration, Ce, and the equilibrium adsorption, Qe, at different temperatures. This was done with the *SciPy* package using the f_oneway module in a *Python* environment. This module uses a one-way ANOVA test to compare the population mean between two or more groups, namely the Ce datasets at different temperatures, as well as the Qe datasets at different temperatures. The null hypothesis for this is that temperature affects Ce and Qe values.

When the values for Ce and Qe were not grouped by temperature, these two datasets had F-statistics of 0.02000 and 0.9961, and p-values of 0.1814 and 0.9085 respectively. Both the F-statistics are low while the p-values are high. This suggests that temperature didn't have a significant effect on the isotherm results, confirming the alternative hypothesis, which corresponds to findings in section 4.2.3.1 which indicate that temperature has a negligible effect on adsorption capacity. This would further indicate that there is a negligible enthalpy of adsorption, which is consistent with observations made by Veenhuyzen et al. (2021), however the reason for this is unclear at this stage. The dataset in its entirety, for all temperatures was thus used for fitting isotherm models.

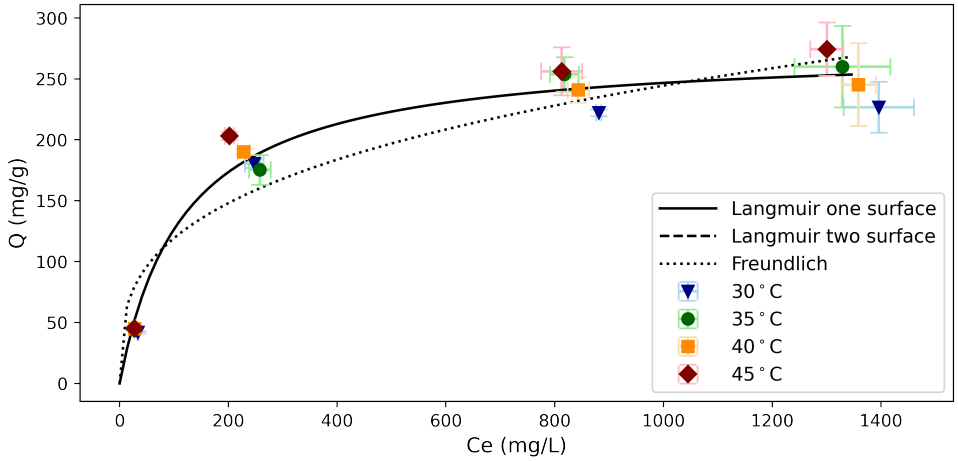

Figure 5.3: Isotherm models fitted to data for 30, 35, 40, and 45 °C data: Langmuir (solid line), Freundlich (dotted line), and two surface Langmuir (dashed line) which converges to the one surface Langmuir isotherm.

Table 5.1: Isotherm results for Langmuir and Freundlich models

Langmuir	$K_L = 0.008479$ (L mg^{-1})	$Q_{max} = 275.82$ (mg g^{-1})	$R^2 = 0.901$
Freundlich	$K_F = 28.39$ (mg g^{-1})(mg L^{-1})$^{\alpha}$	$n = 3.208$	$R^2 = 0.811$
Langmuir	$K_{L,1} = 0.008466$ (L mg^{-1})	$Q_{max,1} = 137.94$ (mg g^{-1})	$R^2 = 0.901$
(two surface)	$K_{L,2} = 0.008466$ (L mg^{-1})	$Q_{max,2} = 137.94$ (mg g^{-1})	

Compared to other fungi, this maximum theoretical adsorption capacity is in the higher range (see table 5.2).

Table 5.2: Isotherm maximum Pb(II) adsorption capacity for some fungal species.

Species	Q_{max} (mg g^{-1})	Isotherm used	Source
Aspergillus caespitosus	351.0	Langmuir	(Aftab et al., 2017)
Aspergillus flavus	346.3	Freundlich	(Aftab et al., 2017)
Aspergillus piperis	275.82	Langmuir	this study
Penicillium sp	60.76 (wet), 52.09 (dry)	Langmuir and Freundlich	(Ezzouhri et al., 2010)
Aspergillus niger	47.62	Langmuir	(Netpae, 2012)
Agaricus bisporus	33.78	Langmuir	(R and Das, 2009)

5.2.2 Kinetic studies

Of the reaction kinetic models (figure 5.4), both the pseudo-first-order (PFO) and two-phase PFO (TP PFO) performed well, however it can be seen that the two surface PFO model has k_f and k_s values that would effectively average to the PFO model values. It is interesting to note that the TP PFO model was fit using a single set of k_f and k_s values for all temperatures, supporting the observation that the system is insensitive to temperature changes. The empirical and Langmuir model results are in table 5.3.

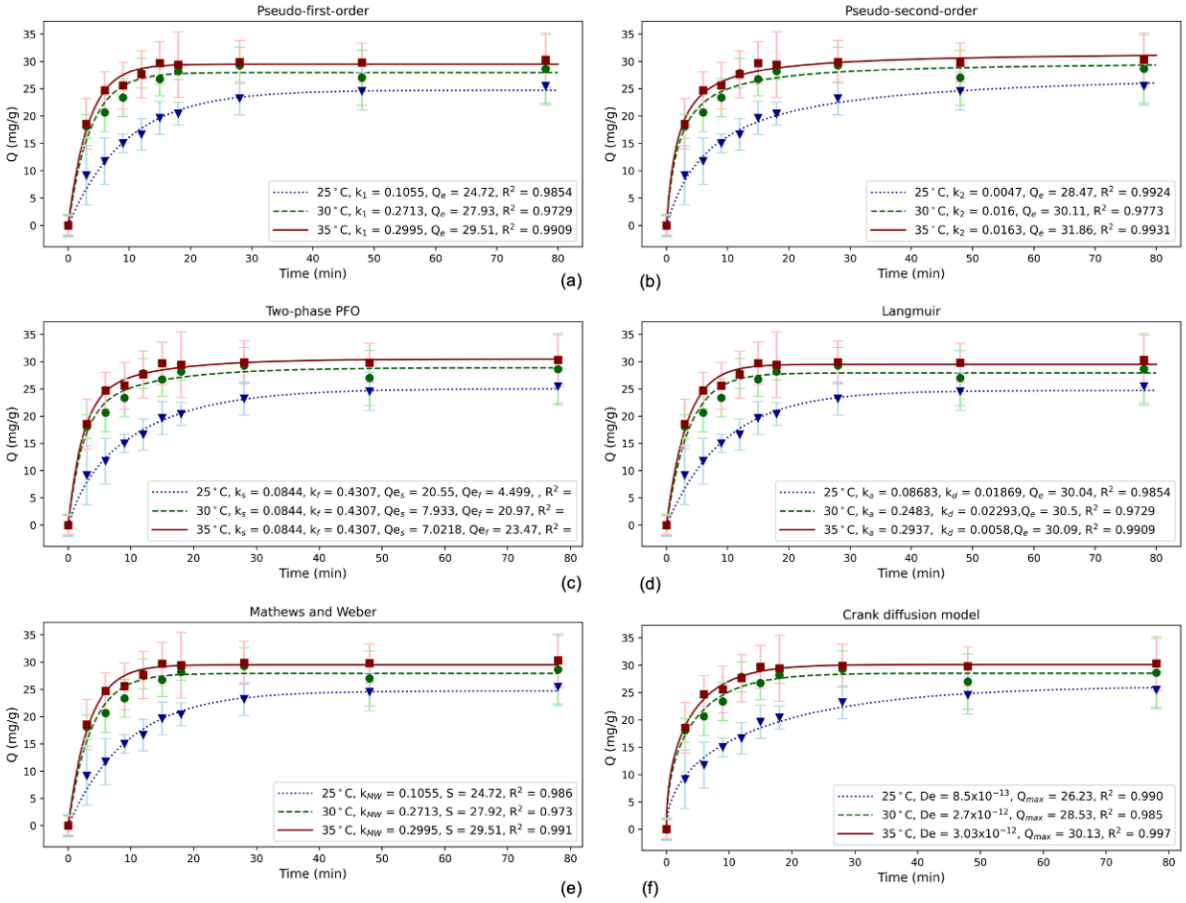

Figure 5.4: Kinetic models considered for the datasets at 25, 30, and 35 °C: (a) Pseudo-first order, (b) pseudo-second order, (c) two-phase PFO, (d) Langmuir, (e) Mathews and Weber, and (f) Crank diffusion model.

The Langmuir kinetic model consistently resulted in a higher adsorption rate constant and lower desorption rate constant across all temperatures, which confirms that the reversible desorption mechanism isn't as powerful as that of adsorption. From the Crank model, the effective diffusivity, D_e, of the adsorbent ranges from 8.5 x10^{-13} to 3.03 x10^{-12} m^2 s^{-1} (table 5.4). Comparing this to the diffusion coefficient of Pb(II) in solution, which is 1.412 x10^{-9} m^2 s^{-1} (Valente et al., 2004), D_e of the biomass is much smaller, which supports the notion that mass transfer effects are dominant in the biomass (Barnes and Turner, 1998). Using Mathews & Weber as well as Crank diffusion models, Biot numbers (table 5.5) at all three temperatures strongly suggest that internal mass transfer (Bi » 100) is the driving force behind the reaction kinetic results.

Table 5.3: Kinetic results for empirical and surface site models.

Model	T (°C)	k (min^{-1}) k_f, k_s (TP) k_a, k_d (Langmuir)	Q_e (mg g^{-1}) $Q_{e,f}$, $Q_{e,s}$ (TP)	R^2
PFO	25	0.1055	24.72	0.985
	30	0.2713	27.93	0.973
	35	0.2995	29.51	0.991
PSO	25	0.0047	28.47	0.992
	30	0.0160	30.11	0.977
	35	0.0163	31.86	0.993
Two-phase (TP)	25	0.4307, 0.0844	4.499, 20.55	0.994
	30	0.4307, 0.0844	20.97, 7.933	0.977
	35	0.4307, 0.0844	23.47, 7.022	0.996
Langmuir	25	0.08683, 0.01869	30.04	0.985
	30	0.2483, 0.02293	30.5	0.973
	35	0.2937, 0.0058	30.09	0.991

Table 5.4: Kinetic results for external and internal mass transfer models.

Model	T (°C)	k (m s^{-1}) (M & W) D_e (m^2 s^{-1}) (Crank)	S (cm^{-1}) (M & W) Q_e (mg g^{-1}) (Crank)	R^2
M & W	25	0.1055	24.72	0.985
	30	0.2713	27.93	0.973
	35	0.2995	29.51	0.991
Crank	25	8.5 x10^{-13}	26.23	0.990
	30	2.7 x10^{-12}	28.53	0.985
	35	3.03 x10^{-12}	30.13	0.997

Table 5.5: External and internal mass transfer results based on Mathews & Weber and Crank models

Temperature (°C)	k_f (m s^{-1})	R^2	Bi
25	5.86 x10^{-5}	0.990	1.38 x10^4
30	1.51 x10^{-4}	0.985	1.10 x10^4
35	1.66 x10^{-4}	0.997	1.10 x10^4

Chapter 6:
Surface Characterisation and Adsorption Mechanism

The aim of this chapter was to develop a potential mechanistic framework that would describe the adsorption data from *Aspergillus piperis* by characterising surface morphologies and composition and comparing the results to literature. This section is based on an extraction of a manuscript published in the journal *Sustainability* in November 2021 (de Wet and Brink, 2021b) with co-author Dr. H.G. Brink.

6.1 FESEM and EDS results

Particle morphology was studied using ultrahigh resolution field emission scanning electron microscopy (FESEM) from Zeiss Ultra Plus55 (Carl Zeiss AG, Oberkochen, Germany) with an InLens detector for high-resolution topographic imaging, an electron high tension of 2 kV acceleration voltage, and a scan speed of 9. The FESEM was then fitted with an energy dispersive X-ray spectrometer (EDS) to identify elemental compositions of specific sites on the mycelium.

FESEM imaging displayed a difference in texture between the biomass before (figure 6.1a) and after (figure 6.1b) adsorption. This could be due to mechanical deformation from re-drying after adsorption. Five locations were selected for EDS spectra analysis pre- and post-adsorption, revealing little or no Pb(II) present before (figure 6.1c) adsorption, and an average of 71.85 wt% after (figure 6.1d) adsorption. EDS mapping (figure 6.2) reveals the elemental distribution of a selected area on the biomass after adsorption. The changes for all major elements present on the adsorbent surface are compared in table 6.1.

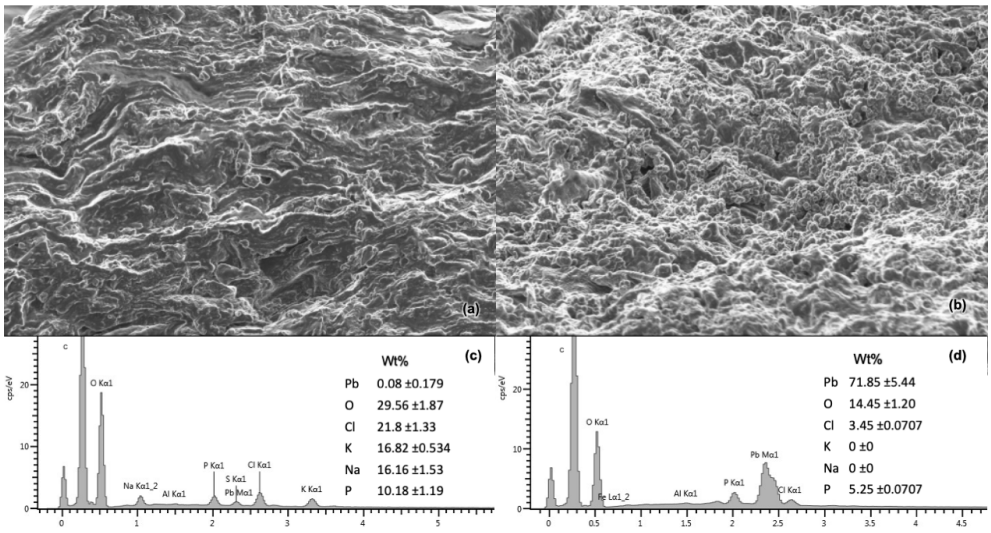

Figure 6.1: FESEM micrograph at 10 000 x magnification (a) before adsorption, (b) after adsorption. EDS spectra (c) before adsorption, (d) after adsorption.

Table 6.1: Average EDS weight percent change at five points for biomass pre- and post-adsorption with standard deviation.

Element	Pre-adsorption wt%	Post-adsorption wt%
Pb	0.08 ±0.179	71.85 ±5.44
O	29.56 ±1.87	14.45 ±1.20
Cl	21.8 ±1.33	3.45 ±0.0707
K	16.82 ±0.534	0.0 ±0.0
Na	16.16 ±1.53	0.0 ±0.0
P	10.18 ±1.19	5.25 ±0.0707

To understand the interaction between the elements, EDS mapping for the pre- and post-adsorption biomass was considered (figure 6.2). An interaction matrix was built using statistical analysis and the software $ImageDiff$ after careful image processing to remove noise such as border pixels, and normalising against a monotone image as described by Muedi et al. (2021). The image pixel distribution was then compared to find overlap between elemental occupation areas to determine which elements are clustered together and consequently imply interaction. These results are reported with standard deviation in tables 6.2 and 6.3.

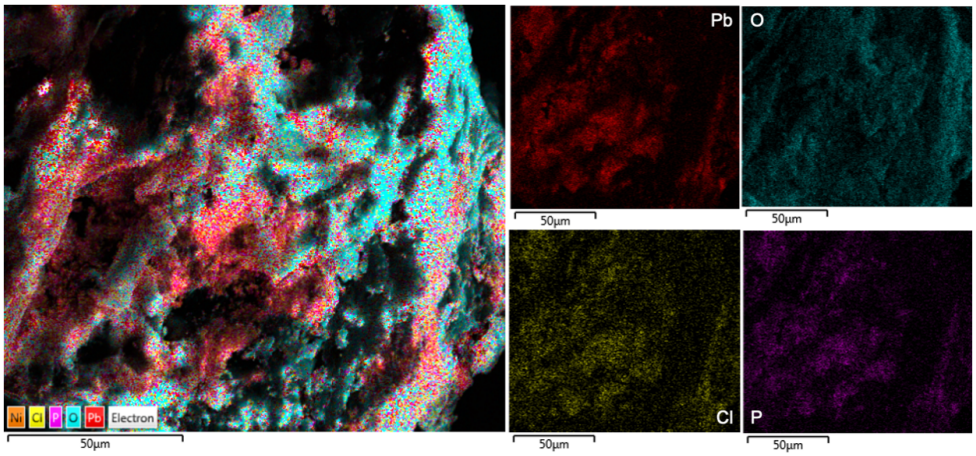

Figure 6.2: EDS mapping of biomass after adsorption

From the interaction matrices, it appears as though there is significant interaction between elements such as sodium and chlorine, potassium and chlorine, and sodium and oxygen before adsorption takes place. Post-adsorption the potassium and sodium ions were completely removed from the surface (tables 6.2 and 6.3). The post adsorption surface indicates strong interactions between Pb(II) and O, and Pb(II) and Cl. This indicates that the Na and K were displaced by the Pb on the surface. It should be noted that even though oxygen shares much of the same regions as Pb(II), there are large areas occupied by O where no Pb(II) is found.

Table 6.2: EDS mapping interaction matrix: Pre-adsorption

	Cl	K	Na	O	P
Cl	100 ±0	87.42 ±16.88	90.09 ±5.13	80.7 ±22.23	73.19 ±34.73
K	87.42 ±16.88	100 ±0	82.67 ±16.28	79.06 ±24.36	73.39 ±32.84
Na	90.09 ±5.13	82.67 ±16.28	100 ±0	81.25 ±18.28	71.9 ±28.99
O	80.7 ±22.23	79.06 ±24.36	81.25 ±18.28	100 ±0	73.19 ±28.09
P	73.19 ±34.73	73.39 ±32.84	71.9 ±28.99	73.19 ±28.09	100 ±0

Table 6.3: EDS mapping interaction matrix: Post-adsorption

	Cl	O	P	Pb
Cl	100 ±0	69.62 ±22.22	77.72 ±8.72	80.69 ±7.82
O	69.62 ±22.22	100 ±0	71.69 ±27.29	74.46 ±33.1
P	77.72 ±8.72	71.69 ±27.29	100 ±0	85.85 ±7.29
Pb	80.69 ±7.82	74.46 ±33.1	85.85 ±7.29	100 ±0

6.2 FTIR results

Fourier transform infrared (FTIR) spectroscopy was recorded on a PerkinElmer Spectrum 2000GX FTIR spectrometer (PerkinElmer, Waltham, USA) used with an attenuated total

reflection attachment (ATR), and recorded at a resolution of 1 cm^{-1} with 32 scans for wavelengths between 4000 and 600 cm^{-1}

FTIR spectra peaks (figure 6.3) indicate OH and NH shifting in the 3260 - 3270 cm^{-1} region and CH stretching in the 2920 - 2930 cm^{-1} region. A shift from 1626.01 to 1643.93 cm^{-1} in the C=C stretching implies that carboxyl groups may be involved in the adsorption process. Larger changes were seen in the shift from 1402.64 to 1538.96 cm^{-1}, implicating that NH deformation may have disappeared and been replaced by OH bending. Additionally, the shift from 1229.04 to 1372.96 cm^{-1} suggests that CN stretching was also involved. Both spectra displayed peaks in the 1020 - 1025 cm^{-1} region which could be attributed to phosphate groups (Jastrzebski et al., 2011).

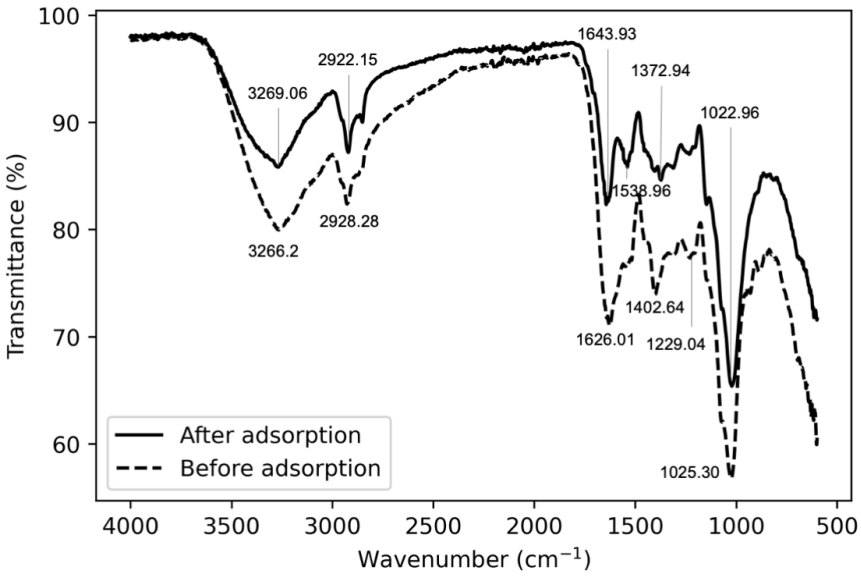

Figure 6.3: FTIR spectra before (dashed line) and after (solid line) adsorption.

6.3 Suggested adsorption mechanisms

To understand what the EDS elemental weight % results mean in terms of molecular amounts, an assumption was made that the oxygen present in the pre- and post-adsorption samples remained constant, and the weight percent for the elements were normalised against this, essentially using 1 wt% O as a basis. After normalisation, the mol percent was calculated for each of the elements to determine the mol fraction change. From this there is a 0.23 mol fraction decrease in Cl and K, and a 0.38 mol fraction decrease in Na, while Pb increased by 0.362 mol fraction. What's notable about this is that the combined decrease in K and Na is roughly double the increase of Pb. This makes sense when considering a simplified version of the ion displacement reaction (S Kumar and Jain, 2013) (equation 6.1), supporting the idea that the K^+ and Na^+ monovalent cations were replaced by Pb^{2+} ions, as was reported by Bairagi et al. (2010).

$$M^{2+}X_2^- + 2N^+ \rightarrow 2N^+X^- + M^{2+} \tag{6.1}$$

In equation 6.1, two salts, MX and NY, react to exchange cations (figure 6.4). In this case M would be Pb^{2+} and N could be either K^+ or Na^+. To further support the argument for cation exchange over other mechanisms, the interaction matrices indicate that oxygen shares only some regions with Pb(II). If factors such as electrostatic forces were driving the adsorption process one would expect to see more overlap between Pb and O.

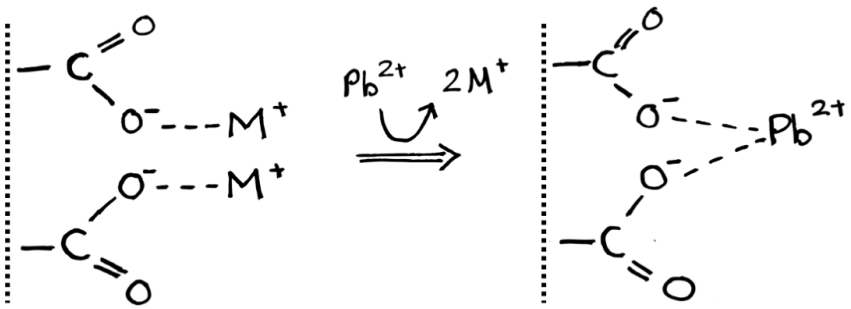

Figure 6.4: Two metal ions, K^+ or Na^+, are replaced by one Pb^{2+} ion.

While it is unclear which exact salts take part in the ion exchange reactions, the FTIR data supports mechanisms seen in literature: The shift from 1626.01 to 1643.93 cm^{-1} suggesting that carboxyl groups may be involved was reported for other species of fungi (Gururajan and Belur, 2018), including *Aspergillus* (Gricajeva et al., 2018). For *Aspergillus piperis* there is always a significant pH drop (on average 26.4 % down to a pH of 2.1, from section 4.2.2.2) that accompanies adsorption, and this could possibly be attributed to hydrogen ion displacement from carboxyl group interactions. The phosphate peaks in the 1020 - 1025 cm^{-1} region alludes to organophosphorus groups that are expected on the biomass and has previously been shown to be involved in adsorption in *Aspergillus versicolor* (Bairagi et al., 2010). These observations provide a strong case for a cation exchange mechanism involving carboxyl and organophosphorus group interactions. Within this context, the findings in section 4.2.3.1 can be explained, where biomass previously exposed to Pb(II) has reduced adsorption capabilities due to the reduction in unoccupied active sites for cation exchange. Additionally, the observed correspondence with the pseudo first order kinetic model as well as the Langmuir isotherm are consistent with the cation exchange of Pb(II) observed by Guo et al. (2013).

Chapter 7:
Conclusion and discussion

This dissertation aimed to answer the research question: **Does *Aspergillus piperis* possess industrially useful Pb(II)-remediation properties?** To explore this question, the fungus' heavy metal tolerance was tested, optimal growth and adsorption conditions were identified, adsorption was quantified through isotherm and kinetic models, and possible adsorption mechanisms were suggested based on surface characterisation.

Heavy Metal Tolerance

Of the metals tested, *A. piperis* only exhibited substantial growth inhibition in Cd(II), while simultaneously completely inhibiting spore formation. Lesser inhibition was observed in Se(IV), Pb(II), and Zn(II) of which the latter two exhibited evidence that additional metal resistance was developed during incubation. After five days the fungus had successfully grown in the presence of all the other metals. The *A. nigri* group is notoriously robust (Ponizovskaya et al., 2017), and extremely ubiquitous (Blackburn, 2006) and *A. piperis* appears to be no exception.

Finding Optimal Growth and Adsorption Conditions

Agar plate experiments revealed that Pb concentration in the PDA has the biggest inhibitory effect on mycelial growth. That said, growth is not fully inhibited, it is only slowed down. Biomass yield using submerged fermentation did not provide clear insight – there were significant fluctuations in mycelium yield and no clear link to initial Pb concentration, the starting pH or incubation temperature. The only factor that consistently resulted in higher yield was increased spore inoculation, which suggests that biomass can be produced under a variety of conditions, provided that there are ample spores available to start the batch fermentation process.

When considering optimal adsorption environments, submerged fermentation experiments indicate that Pb(II) adsorption using live biomass is not only possible but effective, resulting in an average of 82.6% adsorption rate in Pb(II) ranges between 100 and 500 ppm. Sacrificial samples gave insight to the glucose, pH, and biomass weight changes during submerged fermentation. This revealed that glucose depletion takes place after 2.5 days and that trends in the drop of pH follows Pb(II) adsorption closely.

When considering dried biomass adsorption, the biggest effect on adsorption was biomass preprocessing: Biomass exposed to Pb(II) during production, and then nitric acid thereafter performed very poorly compared to control biomass. This was confirmed in the desorption and regeneration studies where desorption of Pb(II) from the biomass is possible using nitric acid, but this destroys the fungus' adsorption capacity thus alternative means of biomass regeneration must be considered. Again this was confirmed in a separate experiment with all other factors kept constant. Optimal pH for adsorption is between 3 and 5, while temperature did not have a significant effect on adsorption.

Adsorption Isotherm and Kinetic Studies

Both the Langmuir isotherm and the two-phase first order models support the observation that the system is relatively insensitive to temperature changes. This bodes well when considering industrial applications as the system would be robust against temperature fluctuations. The Langmuir isotherm model provided the best description of the data suggesting that the system behaves as a homogeneous surface with a monolayer adsorbate. This model produced a K_L of 0.008479 L mg^{-1} and Q_{max} of 275.82 g mg^{-1}, which is relatively high compared to other fungi from the *Aspergillus* genus.

Diffusion kinetics suggest that internal mass transfer is a strong driving force behind kinetic observations, which appear to favour adsorption over desorption as suggested by the Langmuir kinetic model. In addition, this tendency for adsorption rate to be throttled by internal mass transfer could also be due in part to the fibrous nature of the mycelium which inhibits absorption.

Surface Characterisation and Adsorption Mechanism

FESEM imaging displayed expected differences in texture before and after adsorption, which could be attributed to mechanical deformation. EDS confirmed that there was no Pb present on the surface of the samples before adsorption, and that the surface contained 71.85 wt% Pb after adsorption. Oxygen, chlorine and phosphorus wt% dropped after adsorption while sodium and potassium were nearly eliminated from the surface completely. An interaction matrix based on EDS mapping revealed interaction effects between Pb and O and Pb and Cl after adsorption. When this is considered within the context of the stoichiometric changes of Pb, K, and Na, it appears as though K and Na are displaced by Pb. While the salts involved are unknown at this stage, FTIR suggests that carboxyl and organophosphorus group interactions are involved. This potential cation exchange of Na^+ and K^+ is similar to mechanism reported for other members of the *Aspergillus* genus.

Conclusion

From the agar well diffusion studies it is evident that *Aspergillus piperis* not only holds Pb(II)-remediation potential, but could also be utilised in the remediation of other heavy metals. The fungal biomass can be easily and inexpensively propagated in a variety of environments, and adsorption is robust and not notably sensitive to disturbances such as temperature fluctuations. The modelled and experimental adsorption capacities are both

excellent compared to similar fungi and fair well compared to industry practices. All these results indicate that ***A. piperis* would be an excellent candidate for industrial Pb(II)-remediation**.

Although this body of work represents the first time that *A. Piperis* has been studied in the context of remediation, there is still a lot that can be learned from this exciting new fungus. Further studies would explore a system where remediation can take place continuously, and perhaps even *in situ*.

References

Adams, M, MO Moss, and P McClure (2016). *Food Microbiology*. London, UK: The Royal Society of Chemistry. ISBN: 978-1-84973-960-3.

Aftab, K, K Akhtar, R Noreen, F Nazir, and U Kalsoom (Dec. 2017). "Comparative efficacy of locally isolated fungal strains for Pb(II) removal and recovery from water". In: *Chemistry Central Journal* 11.1, p. 133. ISSN: 1752-153X. DOI: 10.1186/s13065-017-0363-4. URL: https://doi.org/10.1186/s13065-017-0363-4.

Akar, T, S Tunali, and AC A (2007). "Study on the characterization of lead (II) biosorption by fungus Aspergillus parasiticus." In: *Applied biochemistry and biotechnology* 136.3. 389, pp. 389–405. ISSN: 0273-2289.

Andrews, P, W Cullen, and E Polishchuk (May 2000). "Arsenic and Antimony Biomethylation by Scopulariopsis brevicaulis: Interaction of Arsenic and Antimony Compounds". In: *Environmental Science and Technology* 34, pp. 324–352. DOI: 10.1021/es991269p.

Atlas, RM and J Philp (2005). *Bioremediation - Applied Microbial Solutions for Real-World Environmental Cleanup*. Washington, DC, USA: American Society for Microbiology. ISBN: 978-1-55581-239-3. URL: https://app.knovel.com/hotlink/toc/id:kpBAMSRWE5/bioremediation-applied/bioremediation-applied.

Babarinde, A, J Babalola, O Adeyemi, and O Oyesiku (Aug. 2010). "Kinetic, Isothermal and Equilibrium Studies of the Biosorption of Pb(II) from Solution by a Moss (Stereophyllum radiculosum)". In: *The Pacific Journal of Science and Technology* 11.12, pp. 29–39.

Bairagi, H, M Khan, L Ray, and A Guha (Nov. 2010). "Adsorption profile of lead on Aspergillus versicolor: A mechanistic probing". In: *Journal of Hazardous Materials* 186, pp. 756–764. DOI: 10.1016/j.jhazmat.2010.11.064.

Bano, A, J Hussain, A Akbar, K Mahmood, M Anwar, M Hasni, S Ullah, S Sajid, and I Ali (Feb. 2018). "Biosorption of heavy metals by obligate halophilic fungi". In: *Chemosphere* 199, p. 13552. DOI: 10.1016/j.chemosphere.2018.02.043.

Barnes, CJ and JV Turner (1998). "Chapter 5 - Isotopic Exchange in Soil Water". In: *Isotope Tracers in Catchment Hydrology*. Ed. by C Kendal and JJ McDonnell. Amsterdam,

the Netherlands: Elsevier, pp. 137–163. ISBN: 978-0-444-81546-0. DOI: https://doi.org/10.1016/B978-0-444-81546-0.50012-4. URL: https://www.sciencedirect.com/science/article/pii/B9780444815460500124.

Berg, H (2015). *Batteries for Electric Vehicles - Materials and Electrochemistry*. Cambridge, UK: Cambridge University Press. ISBN: 978-1-107-08593-0. URL: https://app.knovel.com/hotlink/toc/id:kpBEVME005/batteries-electric-vehicles/batteries-electric-vehicles.

Bhandari, A, RY Surampalli, P Champagne, SK Ong, L Tyagi R. D., and IM C. (2007). *Remediation Technologies for Soils and Groundwater*. Washington, DC, USA: American Society of Civil Engineers (ASCE). ISBN: 978-0-7844-0894-0. URL: https://app.knovel.com/hotlink/toc/id:kpRTSG0007/remediation-technologies/remediation-technologies.

Bhattacharyya, BC and R Banerjee (2007). *Environmental Biotechnology*. Oxford, UK: Oxford University Press. ISBN: 978-0-19-568782-8. URL: https://app.knovel.com/hotlink/toc/id:kpEB000003/environmental-biotechnology/environmental-biotechnology.

Blackburn, C (2006). *Food Spoilage Microorganisms*. Sawston, UK: Woodhead Publishing. ISBN: 978-1-85573-966-6. URL: https://app.knovel.com/hotlink/toc/id:kpFSM00001/food-spoilage-microorganisms/food-spoilage-microorganisms.

Bonev, B, J Hooper, and J Parisot (July 2008). "Principles of assessing bacterial susceptibility to antibiotics using the agar diffusion method". In: *The Journal of antimicrobial chemotherapy* 61, pp. 1295–301. DOI: 10.1093/jac/dkn090.

Boriova, K, S Čerňanský, P Matúš, M Bujdoš, A Simonovicova, and M Urík (Feb. 2019). "Removal of aluminium from aqueous solution by four wild-type strains of Aspergillus niger". In: *Bioprocess and Biosystems Engineering*, pp. 132–155. DOI: 10.1007/s00449-018-2033-x.

Brahmachari, G and JL Demain Arnold L.and Adrio (2017). *Biotechnology of Microbial Enzymes - Production, Biocatalysis and Industrial Applications*. Amsterdam, the Netherlands: Elsevier. ISBN: 978-0-12-803725-6. URL: https://app.knovel.com/hotlink/toc/id:kpBMEPBIA2/biotechnology-microbial/biotechnology-microbial.

Brandl, H (2001). "Heterotrophic leaching". In: *Fungi in bioremediation*. Cambridge, UK: Cambridge University Press, pp. 383–423. ISBN: 9780521781190. DOI: 10.1017/CBO9780511541780.015.

CDC (2012). *Childhood Lead Poisoning Prevention*. URL: https://www.cdc.gov/nceh/lead/data/blood-lead-reference-value.htm (visited on 08/01/2021).

Cecchi, G, A Ceci, P Marescotti, A Persiani, S Piazza, and M Zotti (Mar. 2019). "Interactions among microfungi and pyrite-chalcopyrite mineralizations: tolerance, mineral bioleaching, and metal bioaccumulation". In: *Mycological Progress* 18, pp. 415–423. DOI: 10.1007/s11557-018-01466-y.

Chalad, C, J Kongrueng, K Vongkamjan, WP Robins, V Vuddhakul, and JJ Mekalanos (2018). "Modification of an agar well diffusion technique to isolate yeasts that inhibit Vibrio parahaemolyticus , the causative agent of acute hepatopancreatic necrosis disease". In: *Aquaculture Research*.

Chen, SH, YL Cheow, SL Ng, and A Ting (Sept. 2018). "Mechanisms for metal removal established via electron microscopy and spectroscopy: a case study on metal tolerant fungi Penicillium simplicissimum". In: *Journal of Hazardous Materials* 362, pp. 747–793. DOI: 10.1016/j.jhazmat.2018.08.077.

de Wet, MMM (2019). "Lead mycoremediation potential of Aspergillus piperis: An observational study". In: Unpublished undergraduate report.

de Wet, MMM and HG Brink (2021a). "Chapter 18 - Fungi in the bioremediation of toxic effluents". In: *Fungi Bio-Prospects in Sustainable Agriculture, Environment and Nanotechnology*. Ed. by VK Sharma, MP Shah, S Parmar, and A Kumar. Cambridge, UK: Cambridge Academic Press, pp. 407–431. ISBN: 978-0-12-821925-6. DOI: https://doi.org/10.1016/B978-0-12-821925-6.00018-6. URL: https://www.sciencedirect.com/science/article/pii/B9780128219256000186.

de Wet, MMM and HG Brink (2021b). "Lead Biosorption Characterisation of Aspergillus piperis". In: *Sustainability* 13, p. 13169. DOI: https://doi.org/10.3390/su132313169.

de Wet, MMM, HG Brink, and C Horstmann (Apr. 2020). "Heavy Metal Tolerance of Aspergillus Piperis Using the Agar Well Diffusion Method". In: *Chemical Engineering Transactions* 79, pp. 343–348. DOI: 10.3303/CET2079058.

Doyle, MP and RL Buchanan (2013). *Food Microbiology - Fundamentals and Frontiers (4th Edition)*. Washington, DC, USA: American Society for Microbiology (ASM). ISBN: 978-1-55581-626-1. URL: https://app.knovel.com/hotlink/toc/id:kpFMFFE001/food-microbiology-fundamentals/food-microbiology-fundamentals.

Dynowska, M, K Góralska, G Barańska, P Troska, E Ejdys, E Sucharzewska, and M Tenderenda (Jan. 2011). "Importance of Potato-Dextrose Agar medium in isolation and identification of fungi of the genus Fusarium obtained from clinical materials". In: *Mikologia Lekarska* 18, pp. 119–124.

Ecolab (2018). "Metal Removal". en. In: *Nalco Water Handbook, Fourth Edition*. 4th edition. New York, USA: McGraw-Hill Education. Chap. 25, pp. 239–620. ISBN: 9781259860973. URL: https://www.accessengineeringlibrary.com/content/book/9781259860973/toc-chapter/chapter25/section/section7.

Eldebaiky, S (Oct. 2017). "Antagonistic studies and hyphal interactions of the new antagonist Aspergillus piperis against some phytopathogenic fungi in vitro in comparison with Trichoderma harzianum". In: *Microbial Pathogenesis* 113, pp. 132–165. DOI: 10.1016/j.micpath.2017.10.041.

Eldebaiky, S (May 2018). "Effect of the new antagonist; Aspergillus piperis on germination and growth of tomato plant and Early Blight incidence caused by Alternaria solani". In: *Agricultural Science and Soil Sciences* 6, pp. 41–49.

Espinosa-Ortiz, EJ, E Rene, F Guyot, E van Hullebusch, and P Lens (May 2017). "Biomineralization of tellurium and selenium-tellurium nanoparticles by the white-rot fungus Phanerochaete chrysosporium". In: *International Biodeterioration and Biodegradation* 124, pp. 623–630. DOI: 10.1016/j.ibiod.2017.05.009.

Ezzouhri, L, E Ruiz, E Castro, M Moya, F Espínola, C Lamia, H Er-Raioui, and K Lairini (Jan. 2010). "Mechanisms of lead uptake by fungal biomass isolated from heavy metals habitats". In: *Afinidad* 67, pp. 39–44.

Falkiewicz-Dulik, M, K Janda, and G Wypych (2015). *Handbook of Biodegradation, Biodeterioration, and Biostabilization (2nd Edition)*. Toronto, Canada: ChemTec Publishing. ISBN: 978-1-895198-87-4. URL: https://app.knovel.com/hotlink/toc/id:kpHBBBE005/handbook-biodegradation/handbook-biodegradation.

Filler, DM, I Snape, and DL Barnes (2008). *Bioremediation of Petroleum Hydrocarbons in Cold Regions*. Cambridge, UK: Cambridge University Press. ISBN: 978-0-521-86970-6. URL: https://app.knovel.com/hotlink/toc/id:kpBPHCR005/bioremediation-petroleum/bioremediation-petroleum.

Flickinger, MC (2010). *Encyclopedia of Industrial Biotechnology, Bioprocess, Bioseparation, and Cell Technology, Volumes 1-7*. Hoboken, NJ, USA: John Wiley and Sons. ISBN: 978-0-471-79930-6. URL: https://app.knovel.com/hotlink/toc/id:kpEIBBBCT8/encyclopedia-industrial/encyclopedia-industrial.

Frossard, E, WEH Blum, and BP Warkentin (2006). *Function of Soils for Human Societies and the Environment*. London, UK: Geological Society of London. ISBN: 978-1-86239-207-6. URL: https://app.knovel.com/hotlink/toc/id:kpFSHSE008/function-soils-human/function-soils-human.

Gricajeva, A, S Kazlauskas, L Kalėdienė, and V Bendikienė (2018). "Analysis of Aspergillus sp. lipase immobilization for the application in organic synthesis." In: *International journal of biological macromolecules* 108. 1165, pp. 1165–1175. ISSN: 0141-8130. DOI: 10.1016/j.ijbiomac.2017.11.010. URL: https://doi.org/10.1016/j.ijbiomac.2017.11.010.

Guo, Y Ren, X Sun, Y Xu, X Li, T Zhang, J Kang, and D Liu (2013). "Removal of Pb2+ from aqueous solutions by a high-efficiency resin". In: *Applied Surface Science* 283, pp. 660–667. ISSN: 0169-4332. DOI: https://doi.org/10.1016/j.apsusc.2013.06.161. URL: https://www.sciencedirect.com/science/article/pii/S0169433213012932.

Gupta, V (2016). *New and Future Developments in Microbial Biotechnology and Bioengineering - Microbial Cellulase System Properties and Applications*. Amsterdam, the Netherlands: Elsevier. ISBN: 978-0-444-63507-5. URL: https://app.knovel.com/hotlink/toc/id:kpNFDMBBM1/new-future-developments/new-future-developments.

Gururajan, K and PD Belur (2018). "Screening and selection of indigenous metal tolerant fungal isolates for heavy metal removal". In: *Environmental Technology and Innovation* 9. 91, pp. 91–99. ISSN: 2352-1864. DOI: 10.1016/j.eti.2017.11.001. URL: https://doi.org/10.1016/j.eti.2017.11.001.

Hansda, A, V Kumar, and Anshumali (Aug. 2016). "A comparative review towards potential of microbial cells for heavy metal removal with emphasis on biosorption and bioaccumulation". In: *World Journal of Microbiology and Biotechnology* 32. DOI: 10.1007/s11274-016-2117-1.

Harper, CC, A Mathee, Y von Schirnding, CT De Rosa, and H Falk (2003). "The health impact of environmental pollutants: a special focus on lead exposure in South Africa". In: *International Journal of Hygiene and Environmental Health* 206.4, pp. 315–322. ISSN: 1438-4639. DOI: https://doi.org/10.1078/1438-4639-00227. URL: https://www.sciencedirect.com/science/article/pii/S1438463904702278.

Ho, YS and CF Forster (1996). "Removal of lead ions from aqueous solution using sphagnum moss peat as adsorbent". In: *Water SA* 22.3. 219, pp. 219–224. ISSN: 0378-4738.

Hurst, CJ, RL Crawford, JL Garland, DA Lipson, AL Mills, and LD Stetzenbach (2007). *Manual of Environmental Microbiology (3rd Edition)*. Washington, DC, USA: American Society for Microbiology. ISBN: 978-1-55581-379-6. URL: https://app.knovel.com/hotlink/toc/id:kpMEME0001/manual-environmental/manual-environmental.

Jafarinejad, S (2017). *Petroleum Waste Treatment and Pollution Control*. Amsterdam, the Netherlands: Elsevier. ISBN: 978-0-12-809243-9. URL: https://app.knovel.com/hotlink/toc/id:kpPWTPC00C/petroleum-waste-treatment/petroleum-waste-treatment.

Jastrzebski, W, M Sitarz, M Rokita, and K Bulat (2011). "Infrared spectroscopy of different phosphates structures". In: *Spectrochimica Acta Part A: Molecular and Biomolecular Spectroscopy* 79.4. The Xth International Conference on Molecular Spectroscopy, pp. 722–727. ISSN: 1386-1425. DOI: https://doi.org/10.1016/j.saa.2010.08.044. URL: https://www.sciencedirect.com/science/article/pii/S1386142510004348.

Ji, Z, C Feng, X Wu, Y Li, L Li, and X Liu (2017). "Composite of biomass and lead resistent Aspergillus oryzae for highly efficient aqueous phase Pb(II) adsorption". In: *Environmental Progress and Sustainable Energy* 36.6. 1658, pp. 1658–1666. ISSN: 1944-7442. DOI: 10.1002/ep.12623. URL: https://doi.org/10.1002/ep.12623.

Joshi, P, A Swarup, S Maheshwari, R Kumar, and N Singh (Oct. 2011). "Bioremediation of Heavy Metals in Liquid Media Through Fungi Isolated from Contaminated Sources". In: *Indian journal of microbiology* 51, pp. 482–7. DOI: 10.1007/s12088-011-0110-9.

Jovicic-Petrovic, J, S Jeremic, I Vuckovic, S Vojnović, A Bulajić, V Raicevic, and J Nikodinovic-Runic (Jan. 2016). "Aspergillus piperis A/5 from plum-distilling waste compost produces a complex of antifungal metabolites active against the phytopathogen

Pythium aphanidermatum". In: *Archives of Biological Sciences* 68, pp. 16–16. DOI: 10.2298/ABS150602016J.

Kapoor, A and T Viraraghavan (1995). "Fungal biosorption — an alternative treatment option for heavy metal bearing wastewaters: a review". In: *Bioresource Technology* 53.3, pp. 195–206. ISSN: 0960-8524. DOI: https://doi.org/10.1016/0960-8524(95)00072-M. URL: https://www.sciencedirect.com/science/article/pii/096085249500072M.

Kariuki, Z, J Kiptoo, and D Onyancha (Feb. 2017). "Biosorption studies of lead and copper using rogers mushroom biomass 'Lepiota Hystrix'". In: *South African Journal of Chemical Engineering* 23, pp. 472–499. DOI: 10.1016/j.sajce.2017.02.001.

Khan, I, M Aftab, S Shakir, M Ali, S Qayyum, M Rehman, K Haleem, and I Touseef (2019). "Mycoremediation of heavy metal (Cd and Cr)-polluted soil through indigenous metallotolerant fungal isolates". In: *Environmental Monitoring and Assessment : An International Journal Devoted to Progress in the Use of Monitoring Data in Assessing Environmental Risks to Man and the Environment* 191.9. 1, pp. 1–11. ISSN: 0167-6369. DOI: 10.1007/s10661-019-7769-5. URL: https://doi.org/10.1007/s10661-019-7769-5.

Kück, U and N Frankenberg-Dinkel (2015). *Biotechnology*. De Gruyter. ISBN: 978-3-11-034110-2. URL: https://app.knovel.com/hotlink/toc/id:kpB0000011/biotechnology/biotechnology.

Kumar, M, M Pallapothu, H Sarnaik, and A Sadhukhan (Apr. 2000). "A rapid technique for screening of lovastatin-producing strains of Aspergillus terreus by agar plug and Neurospora crassa bioassay". In: *Journal of microbiological methods* 40, pp. 99–104. DOI: 10.1016/S0167-7012(99)00135-9.

Kumar, S and S Jain (Oct. 2013). "History, Introduction, and Kinetics of Ion Exchange Materials". In: *Journal of Chemistry* 2013, pp. 385–396. DOI: 10.1155/2013/957647.

Largitte, L and R Pasquier (2016). "A review of the kinetics adsorption models and their application to the adsorption of lead by an activated carbon". In: *Chemical Engineering Research and Design* 109, pp. 495–504. ISSN: 0263-8762. DOI: https://doi.org/10.1016/j.cherd.2016.02.006. URL: https://www.sciencedirect.com/science/article/pii/S0263876216000691.

Lehr, J, J Keeley, and J Lehr (2005). *Water Encyclopedia, Volumes 1-5*. Hoboken, NJ, USA: John Wiley and Sons. ISBN: 978-0-471-44164-9. URL: https://app.knovel.com/hotlink/toc/id:kpWEV00004/water-encyclopedia-volumes/water-encyclopedia-volumes.

Li, Q and G Gadd (Oct. 2017). "Biosynthesis of copper carbonate nanoparticles by ureolytic fungi". In: *Applied Microbiology and Biotechnology* 101, p. 16558. DOI: 10.1007/s00253-017-8451-x.

Lochner, R and J Matar (1990). *Designing for Quality: An introduction to the best of Taguchi and Western methods of statistical experimental design*. Amsterdam, the Netherlands: Springer. ISBN: 978-0-412-40020-9.

Lu, L (2015). *Iron Ore - Mineralogy, Processing and Environmental Sustainability*. Amsterdam, the Netherlands: Elsevier. ISBN: 978-1-78242-156-6. URL: https://app.knovel.com/hotlink/toc/id:kpIOMPES01/iron-ore-mineralogy-processing/iron-ore-mineralogy-processing.

Mackenzie, L and P Davis (2020). *Water and Wastewater Engineering: Design Principles and Practice, Second Edition*. en. 2nd edition. New York, USA: McGraw-Hill Education. ISBN: 9781260132274. URL: https://www.accessengineeringlibrary.com/content/book/9781260132274.

Manivasakam, N (2016). *Industrial Effluents - Origin, Characteristics, Effects, Analysis and Treatment*. Los Angeles, CA, USA: Chemical Publishing Company Inc. ISBN: 978-08206-0414-5. URL: https://app.knovel.com/hotlink/toc/id:kpIEOCEAT3/industrial-effluents/industrial-effluents.

Marafi, M, A Stanislaus, and E Furimsky (2017). *Handbook of Spent Hydroprocessing Catalysts (2nd Edition)*. Amsterdam, the Netherlands: Elsevier. ISBN: 978-0-44-463881-6. URL: https://app.knovel.com/hotlink/toc/id:kpHSHCE005/handbook-spent-hydroprocessing/handbook-spent-hydroprocessing.

Marappa, N, D Dharumadurai, V Gopal, and N Thajuddin (June 2017). "Extraction and recovery of precious metals from electronic waste printed circuit boards by bioleaching acidophilic fungi". In: *International journal of Environmental Science and Technology* 15, pp. 42–68. DOI: 10.1007/s13762-017-1372-5.

Mathee, A (2014). "Towards the prevention of lead exposure in South Africa: Contemporary and emerging challenges". In: *NeuroToxicology* 45, pp. 220–223. ISSN: 0161-813X. DOI: https://doi.org/10.1016/j.neuro.2014.07.007. URL: https://www.sciencedirect.com/science/article/pii/S0161813X14001363.

Mathew, B, K Beeregowda, and T Krishnamurthy (Jan. 2015). "Bioaccumulation of Heavy Metals by Fungi". In: *International journal of environmental chemistry and chromatography* 1, pp. 15–21.

Muedi, K, H Brink, V Masindi, and J Maree (2021). "Effective removal of arsenate from wastewater using aluminium enriched ferric oxide-hydroxide recovered from authentic acid mine drainage". In: *Journal of Hazardous Materials* 414, p. 125491. ISSN: 0304-3894. DOI: https://doi.org/10.1016/j.jhazmat.2021.125491. URL: https://www.sciencedirect.com/science/article/pii/S0304389421004544.

Naidu, R, E Smith, G Owens, P Bhattacharya, and P Nadebaum (2006). *Managing Arsenic in the Environment - From Soil to Human Health*. Victoria, Australia: CSIRO Publishing. ISBN: 978-1-57808-425-8. URL: https://app.knovel.com/hotlink/toc/id:kpMAEFSHH1/managing-arsenic-in-environment/managing-arsenic-in-environment.

NCBI (2017). *Lovastatin*. URL: https://www.ncbi.nlm.nih.gov/books/NBK548670/ (visited on 02/02/2020).

Netpae, T (2012). "Removal of Lead from Aqueous Solutions by Aspergillus niger from Artificial Vinegar Factory". In: *Electronic Journal of Biology* 8.

Ngo, H, W Guo, R Surampalli, and T Zhang (2016). *Green Technologies for Sustainable Water Management*. URL: https://app.knovel.com/hotlink/khtml/id:kt0113G0W1/green-technologies-sustainable/biosorption.

Onami, Ji, M Watanabe, T Yoshinari, R Hashimoto, M Kitayama, N Kobayashi, Y Sugita-Konishi, Y Kamata, H Takahashi, and J Terajima (June 2018). "Fumonisin-production by Aspergillus section Nigri isolates from Japanese Foods and Environments". In: *Food Safety* 6, pp. 74–82. DOI: 10.14252/foodsafetyfscj.2018005.

Paco, A, K Duarte, J Da Costa, P Santos, R Pereira, M Pereira, A Freitas, A Duarte, and T Rocha-Santos (May 2017). "Biodegradation of polyethylene microplastics by the marine fungus Zalerion maritimum". In: *Science of The Total Environment* 586, pp. 10–15. DOI: 10.1016/j.scitotenv.2017.02.017.

Pandey, A, C Larroche, CG Dussap, E Gnansounou, SK Khanal, and S Ricke (2019). *Biomass, Biofuels, Biochemicals - Biofuels - Alternative Feedstocks and Conversion Processes for the Production of Liquid and Gaseous Biofuels (2nd Edition)*. Amsterdam, the Netherlands: Elsevier. ISBN: 978-0-1281-6856-1. URL: https://app.knovel.com/hotlink/toc/id:kpBBBBAFC3/biomass-biofuels-biochemicals/biomass-biofuels-biochemicals.

Peens, J (2018). "Pb(II) Removal From Water Using Microorganisms Evolved to Tolerate Pb(II) Toxicity". unpublished thesis. MA thesis. University of Pretoria.

Ponizovskaya, VB, MY Dyakov, AB Antropova, EN Bilanenko, VL Mokeeva, and VK Ilyin (2017). "The survival of micromycetes exposed to space conditions". In: *Moscow University Biological Sciences Bulletin* 72, pp. 6–12.

Prasad, R and S Srivastava (Jan. 2009). "Sorption of distillery spent wash onto fly ash: Kinetics and mass transfer studies". In: *Chemical Engineering Journal* 146, pp. 90–97. DOI: 10.1016/j.cej.2008.05.021.

Price, M, J Classen, and G Payne (Apr. 2001). "Aspergillus niger Absorbs Copper and Zinc from Swine Waste Water". In: *Bioresource technology* 77, pp. 41–9. DOI: 10.1016/S0960-8524(00)00135-8.

Priyadarshini, E, S Priyadarshini, and N Pradhan (2019). "Heavy metal resistance in algae and its application for metal nanoparticle synthesis". In: *Applied Microbiology and Biotechnology* 103.8. 3297, pp. 3297–3316. ISSN: 0175-7598. DOI: 10.1007/s00253-019-09685-3. URL: https://doi.org/10.1007/s00253-019-09685-3.

Priyadarshini, E, S Priyadarshini, B Cousins, and N Pradhan (2021). "Metal-Fungus interaction: Review on cellular processes underlying heavy metal detoxification and synthesis of metal nanoparticles". In: *Chemosphere* 274, pp. 129–176. ISSN: 0045-6535. DOI: 10.1016/j.chemosphere.2021.129976. URL: https://doi.org/10.1016/j.chemosphere.2021.129976.

R, V and N Das (Aug. 2009). "Biosorption of Cadmium (II) and Lead (II) From Aqueous Solutions Using Mushrooms: A Comparative Study". In: *Journal of Hazardous Materials* 168, pp. 376–382. DOI: 10.1016/j.jhazmat.2009.02.062.

Rathoure, AK and VK Dhatwalia (2016). *Toxicity and Waste Management Using Bioremediation*. Hershey, PA, USA: IGI Global. ISBN: 978-1-4666-9734-8. URL: https://app.knovel.com/hotlink/toc/id:kpTWMUB003/toxicity-waste-management/toxicity-waste-management.

Robinson, RK (2000). *Encyclopedia of Food Microbiology, Volumes 1-3*. Amsterdam, the Netherlands: Elsevier. ISBN: 978-0-12-227070-3. URL: https://app.knovel.com/hotlink/toc/id:kpEFMV0004/encyclopedia-food-microbiology/encyclopedia-food-microbiology.

Rybczynska-Tkaczyk, K and T Korniłłowicz-Kowalska (Sept. 2016). "Biosorption optimization and equilibrium isotherm of industrial dye compounds in novel strains of microscopic fungi". In: *International journal of Environmental Science and Technology* 13, pp. 2837–2846. DOI: 10.1007/s13762-016-1111-3.

Sahoo, TR and B Prelot (2020). "Chapter 7 - Adsorption processes for the removal of contaminants from wastewater: the perspective role of nanomaterials and nanotechnology". In: *Nanomaterials for the Detection and Removal of Wastewater Pollutants*. Ed. by B Bonelli, FS Freyria, I Rossetti, and R Sethi. Micro and Nano Technologies. Amsterdam, the Netherlands: Elsevier, pp. 161–222. ISBN: 978-0-12-818489-9. DOI: https://doi.org/10.1016/B978-0-12-818489-9.00007-4. URL: https://www.sciencedirect.com/science/article/pii/B9780128184899000074.

Al-Salem, S (2019). *Plastics to Energy: Fuel, Chemicals and Sustainability Implications*. Amsterdam, the Netherlands: Elsivier, p. 1567. ISBN: 978-0-12-813140-4.

Samson, RA, J Houbraken, AFA Kuijpers, JM Frank, and JC Frisvad (2004). "New ochratoxin A or sclerotium producing species in Aspergillus section Nigri." In: *Studies in Mycology* 50, pp. 45–61.

Sao, K, M Pandey, PK Pandey, and F Khan (Aug. 2017). "Highly efficient biosorptive removal of lead from industrial effluent". In: *Environmental Science and Pollution Research* 24.22, pp. 18410–18420. ISSN: 1614-7499. DOI: 10.1007/s11356-017-9413-7. URL: https://doi.org/10.1007/s11356-017-9413-7.

Shah, A, V Maurya, C Panjabi, and P Khanna (Mar. 2004). "Allergic bronchopulmonary aspergillosis without clinical asthma caused by Aspergillus niger". In: *Allergy* 59, pp. 236–7. DOI: 10.1046/j.1398-9995.2003.00372.x.

Show, PL, K Oladele, QY Siew, F Zakry, J Lan, and T Ling (Apr. 2015). "Overview of citric acid production from Aspergillus niger". In: *Frontiers in Life Science* 8, pp. 1–13. DOI: 10.1080/21553769.2015.1033653.

Soleimani, M, M Hajabbasi, A Majid, A Mirlohi, O Borggaard, and P Holm (Aug. 2010). "Effect of Endophytic Fungi on Cadmium Tolerance and Bioaccumulation by Festuca Arundinacea and Festuca Pratensis". In: *International journal of phytoremediation* 12, pp. 535–49. DOI: 10.1080/15226510903353187.

Stamets, P (2005). *Mycelium Running: How Mushrooms Can Help Save the World*. Berkley, CA, USA: Ten Speed Press. ISBN: 9781580085793. URL: https://books.google.co.za/books?id=NPI8%5C_-omzvsC.

Tang, A, Y Lu, Q Li, X Zhang, N Cheng, H Liu, and Y Liu (2021). "Simultaneous leaching of multiple heavy metals from a soil column by extracellular polymeric substances of Aspergillus tubingensis F12". In: *Chemosphere* 263, p. 127883. ISSN: 0045-6535. DOI: https://doi.org/10.1016/j.chemosphere.2020.127883. URL: https://www.sciencedirect.com/science/article/pii/S0045653520320786.

Vale, S (Mar. 2016). "Cr and Zn biosorption by Aspergillus niger". In: *Environmental Earth Sciences* 75, pp. 1–11.

Valente, AJM, ACF Ribeiro, VM Lobo, and A Jiménez (2004). "Diffusion coefficients of lead (II) nitrate in nitric acid aqueous solutions at 298 K". In: *Journal of Molecular Liquids* 111, pp. 33–38.

Varga, J, J Frisvad, S Kocsubé, B Brankovics, B Tóth, G Szigeti, and R Samson (June 2011). "New and revisited species in Aspergillus section Nigri". In: *Studies in mycology* 69, pp. 1–17. DOI: 10.3114/sim.2011.69.01.

Veenhuyzen, B van, S Tichapondwa, C Cilliers, E Chirwa, and H Brink (Apr. 2021). "High Capacity Pb(II) Adsorption Characteristics onto Raw- and Chemically Activated Waste Activated Sludge". In: *Journal of Hazardous Materials* 416, p. 125943. DOI: 10.1016/j.jhazmat.2021.125943.

Vesth, T, J Nybo, S Theobald, J Frisvad, TO Larsen, K Nielsen, J Hoof, J Brandl, A Salamov, R Riley, J Gladden, P Phatale, M Nielsen, E Lyhne, M Kogle, K Strasser, E Mcdonnell, K Barry, A Clum, and M Andersen (Dec. 2018). "Investigation of inter- and intraspecies variation through genome sequencing of Aspergillus section Nigri". In: *Nature Genetics* 50, pp. 13–27. DOI: 10.1038/s41588-018-0246-1.

Wang, J and X Guo (2020). "Adsorption kinetic models: Physical meanings, applications, and solving methods". In: *Journal of Hazardous Materials* 390, p. 122156. ISSN: 0304-3894. DOI: https://doi.org/10.1016/j.jhazmat.2020.122156. URL: https://www.sciencedirect.com/science/article/pii/S0304389420301448.

WEF (2017). *Wastewater Biology - The Microlife (3rd Edition)*. WEF. ISBN: 978-1-57278-337-9. URL: https://app.knovel.com/hotlink/toc/id:kpWBTME011/wastewater-biology-microlife/wastewater-biology-microlife.

Wei, J, M Duan, Y Li, A Nwankwegu, Y Ji, and J Zhang (Sept. 2019). "Concentration and pollution assessment of heavy metals within surface sediments of the Raohe Basin, China". In: *Scientific Reports* 9, pp. 1–7. DOI: 10.1038/s41598-019-49724-7.

Xie, ZP, ZN Xu, WH Shen, and PL Cen (Dec. 2005). "Bioassay of Mildiomycin and a Rapid, Cost-Effective Agar Plug Method for Screening High-yielding Mutants of Mildiomycin". In: *World Journal of Microbiology and Biotechnology* 21.8, pp. 1433–1437. ISSN: 1573-0972. DOI: 10.1007/s11274-005-6561-6. URL: https://doi.org/10.1007/s11274-005-6561-6.

Yates, MV, CH Nakatsu, RV Miller, and SD Pillai (2016). *Manual of Environmental Microbiology (4th Edition)*. Washington, DC, USA: American Society for Microbiology. ISBN: 978-1-55581-602-5. URL: https://app.knovel.com/hotlink/toc/id:kpMEME0014/manual-environmental/manual-environmental.

Yousefi, N, M Jones, A Bismarck, and A Mautner (2021). "Fungal chitin-glucan nanopapers with heavy metal adsorption properties for ultrafiltration of organic solvents and water." In: *Carbohydrate polymers* 253. 117273, p. 117273. ISSN: 0144-8617. DOI: 10.1016/j.carbpol.2020.117273. URL: https://doi.org/10.1016/j.carbpol.2020.117273.

Zaidi, A, P Wani, and M Khan (Jan. 2012). *Toxicity of Heavy Metals to Legumes and Bioremediation*, pp. 122–138. ISBN: 978-3-7091-0729-4. DOI: 10.1007/978-3-7091-0730-0.

Zhou, L and D Li (2018). "Adsorption of heavy metal tolerance strains to Pb2+ and Cd2+ in wastewater". In: *Environmental Science and Pollution Research* 25.32. 32156, pp. 32156–32162. ISSN: 0944-1344. DOI: 10.1007/s11356-018-2988-9. URL: https://doi.org/10.1007/s11356-018-2988-9.